Journal of Mammalian Evolution (2022) 29:207–235
https://doi.org/10.1007/s10914-021-09567-4

ORIGINAL PAPER

Postcranial Morphology of the Extinct Rodent *Neoepiblema* (Rodentia: Chinchilloidea): Insights Into the Paleobiology of Neoepiblemids

Leonardo Kerber[1,2,3] · Adriana M. Candela[4] · José Darival Ferreira[2] · Flávio A. Pretto[1,2] · Jamile Bubadué[5] · Francisco R. Negri[6]

Accepted: 1 August 2021 / Published online: 19 October 2021

Abstract

In this paper, we study the postcranial morphology (humerus, ulna, innominate, femur, tibia, astragalus, navicular, and metatarsal III) of *Neoepiblema*, a giant Late Miocene South American rodent, searching for evidence about its paleobiology based on unpublished specimens from Solimões Formation (Upper Miocene, Brazil). The study includes a morphofunctional analysis of the postcranial bones and a comparison with extant and extinct rodents, especially *Phoberomys*. The morphofunctional analysis of the postcranial bones suggests that *Neoepiblema* (as well as *Phoberomys*) would have a crouched forelimb that was not fully extended, with powerful pectoral and triceps musculature, and able to produce movements of pronation/supination and possibly with a hand able to grasp. The combination of characters of the innominate bone, femur, and tibia indicates a predominance of parasagittal movements and a thigh with powerful musculature used during propulsion. In sum, the analyzed postcranial features are consistent with the limb morphology of ambulatory rodents, but with faculty to dig or swim. The sedimentary evidence of the localities in which fossils of neoepiblemids have been found suggests that these rodents lived in wet and water-related environments (near swamps, lakes, and/or rivers).

Keywords Giant rodents · Functional morphology · Neogene · Neoepiblemidae · Solimões Formation

Introduction

Neoepiblemids are caviomorph rodents (South American hystricognath rodents; see Vucetich et al. 2015, for a review on the caviomorph fossil record) represented by only four genera, but with a wide range of body sizes. This lineage represents a group more closely related to extant Chinchillidae than to other caviomorph clades (Kerber et al. 2017a, b; Rasia and Candela 2018, 2019; Kerber and Sánchez-Villagra 2019; Busker et al. 2020; Rasia et al. 2021) (Fig. 1). They are unequivocally recorded from the Early Miocene to the Pliocene of South America (see Discussion) and are represented by *Perimys* Ameghino, 1887 (including several species) (Early Miocene), *Doryperimys olsacheri* Kramarz et al., 2015 (Early Miocene), *Neoepiblema horridula* (Ameghino, 1886) (Late Miocene), *Neoepiblema acreensis* Bocquentin-Villanueva et al., 1990 (Late Miocene), *Phoberomys burmeisteri* Kraglievich, 1926 (Late Miocene), and *Phoberomys pattersoni* Mones, 1980 (Late Miocene) (Kraglievich 1926, 1940; Bondesio et al. 1975; Carrillo and Sánchez-Villagra 2015; Kerber et al. 2017a, b; 2019a, b; Rasia and Candela 2018, 2019).

✉ Leonardo Kerber
leonardokerber@gmail.com

1 Centro de Apoio à Pesquisa Paleontológica da Quarta Colônia, Universidade Federal de Santa Maria, Rua Maximiliano Vizzotto, 598, São João do Polêsine 97230–000, Brazil

2 Programa de Pós-Graduação em Biodiversidade Animal, Centro de Ciências Naturais e Exatas, Universidade Federal de Santa Maria, Av. Roraima nº 1000, Santa Maria 97105-900, Brazil

3 Museu Paraense Emílio Goeldi, Coordenação de Ciências da Terra e Ecologia, Av. 19 Perimetral, 1901, Belém 66077–830, Brazil

4 CONICET, División Paleontología Vertebrados, Museo de La Plata, Paseo del Bosque, s/n, La Plata, B1900FWA La Plata, Argentina

5 Laboratório de Ciências Ambientais, Universidade Estadual Do Norte Fluminense, Av. Alberto Lamego, Campos dos Goytacazes 875, 28013-602, Brazil

6 Laboratório de Paleontologia, Universidade Federal do Acre (Campus Floresta), Rua Estrada da Canela Fina, KM 12, Cruzeiro do Sul, Acre 69980-000, Brazil

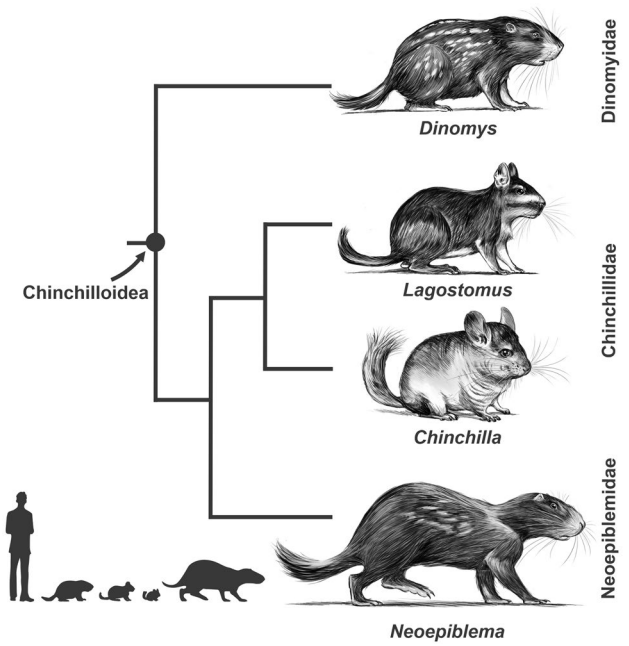

Fig. 1 Simplified cladogram of Chinchilloidea showing the phylogenetic relationships of *Neoepiblema* and extant chinchilloids. Based on Kerber et al. (2017a, 2019a), Kerber and Sánchez-Villagra (2019), Rasia and Candela (2018, 2019), Rasia et al. (2021). Illustration of rodents by Márcio L. Castro

Although our knowledge of the anatomy of the members of this group has been increasing in recent years, it is still far from ideal, making it challenging to understand their phylogenetic relationships as well as their paleobiology. Most information about neoepiblemids is based on the morphology of the skull and cheek teeth. Among the aforementioned species, there is information about the postcranial morphology only of *P. burmeisteri*, *P. pattersoni*, and *Perimys* (see below). A few bones (femur, tibia, and astragalus) from the Ituzaingó Formation, Argentina, were described by the Argentinean paleontologist Lucas Kraglievich. These bones were assigned to *Phoberomys burmeisteri*, the giant Miocene Argentinean form (Kraglievich 1932). Subsequently, a femur assigned to *P. burmeisteri* from Juruá River, Solimões Formation, Brazil, was described by Paula Couto (1978). Kerber et al. (2017a) argued that, at present, there is no specimen of *Phoberomys* from Brazil that can be identified confidently at a specific level. Hence, that femur is now assigned to *Phoberomys* sp. instead. In the early 2000s, an almost complete but poorly preserved skeleton of *Phoberomys pattersoni* was found in the Urumaco Formation of Venezuela, including postcranial remains associated with the skull (Sánchez–Villagra et al. 2003; Horovitz et al. 2006; see also Geiger et al. 2013). More recently, Muñoz et al. (2019) described the forelimb bones of *Perimys* from the Santa Cruz Formation, Argentina.

The analysis of postcranial features can furnish phylogenetic information (Horovitz et al. 2006; Weisbecker and Schimid 2006) and data for interpretation of the locomotor habits of extinct mammals, contributing to the understanding of their paleobiology (Van Valkenburgh 1987). Although extant caviomorphs have diverse locomotor habits, and recent approaches have provided an important characterization of ecomorphological patterns that can be applied to the reconstruction of the habits of extinct species (e.g., Elissamburu and Vizcaíno 2004; Morgan and Verzi 2006; Weisbecker and Schimid 2006; Rocha-Barbosa et al. 2007; Samuels and Van Valkenburgh 2008; Morgan 2009; García–Esponda and Candela 2010, 2016; Wilson and Geiger 2015; Ginot et al. 2016; Candela et al. 2017; García-Esponda et al. 2021), few studies have focused on making inferences about the locomotor habits and other paleobiological aspects of extinct South American rodents (e.g., Biknevicius 1993; Biknevicius et al. 1993; Candela and Picasso 2008; Candela et al. 2012, 2018; Geiger et al. 2013; Wilson and Geiger 2015; Muñoz et al. 2019).

In recent contributions, the morphology of the skull and teeth and their implications for taxonomy, phylogeny, and paleobiology of Brazilian Late Miocene neoepiblemids have been studied (Kerber et al. 2017a, b; 2019a, b; Ferreira et al. 2020). Inferences, mainly based on the paleobiogeographic and sedimentary patterns of the neoepiblemid fossils, but also based on osteological traits, have suggested that they probably inhabited water-related environments, like swamps, lakes, or rivers, being possibly semiaquatic or using these places to forage (Sánchez-Villagra et al. 2003; Vucetich et al. 2010; Nasif et al. 2013; Wilson and Geiger 2015; Kerber et al. 2017b). In this paper, we analyze the morphology of postcranial bones of *Neoepiblema* (with an emphasis on *N. acreensis*, the best-sampled neoepiblemid from Brazil). We discuss their morphofunctional implications and body mass estimates, furnishing paleobiological evidence about these rodents.

Material and Methods

Methodology

The anatomical description of the postcranial bones is based on the better-preserved specimens. The materials analyzed here are assigned to two species: *N. acreensis* and *N. horridula*. The osteology of both species is similar, differing mainly in the larger size and robustness of *N. acreensis*. The specimens were found in the fossiliferous sites Niterói, Patos (Acre River), and Talismã (Purus River) from Solimões Formation (Upper Miocene), Brazil (see below). The specimens from Niterói are assigned to *N. acreensis* and specimens from Talismã locality to *N. horridula*, following Kerber

et al. (2017a, b; 2019a, b), who previously described several specimens (craniodental remains) from these localities. The specimen from Patos locality is tentatively assigned to *N. acreensis*, based on the morphological and size similarity with the Niterói material. No collection data are available to indicate whether the specimens were found directly associated with cranial and dentary remains of *Neoepiblema,* but they were collected in the same levels where several remains of these rodents have been found (Negri and Ferigolo 1999; Kerber et al. 2017a, b; 2019a, b). Besides, the specimens have proportional sizes to the craniodental remains of both *Neoepiblema* species.

For comparison, we examined specimens of the extant caviomorphs *Chinchilla lanigera, Lagostomus maximus, Cavia aperea, Myocastor coypus,* and *Coendou spinosus* (unnumbered specimens of CAPPA/UFSM-AC), which exhibit a wide array of locomotor behaviors and substrate preferences (e.g., Candela et al. 2017: table 1). The postcranial anatomy of extant species was also evaluated from bibliographic sources (e.g., Mones 1997; Candela and Picasso 2008; Araújo et al. 2013; Ginot et al. 2016; Candela et al. 2017). Comparative studies of extinct caviomorphs included first-hand observation of postcranial bones of the neoepiblemid *Phoberomys burmeisteri* (MACN 3344, MACN 3147; Ituzaingó Formation, Upper Miocene, Argentina) and *Phoberomys* sp. (DGM 601-M, Solimões Formation, Upper Miocene, Brazil). *Phoberomys pattersoni* (UNEFM–VF–20; Urumaco Formation, Upper Miocene, Venezuela) was studied from additional images provided by the authors of the specimen description (Sánchez-Villagra et al. 2003; Horovitz et al. 2006). Analysis of the Miocene neoepiblemid *Perimys* was based on data provided by Muñoz et al. (2019). Information on the other extinct lineages of caviomorphs was taken from published sources (Candela and Picasso 2008; Candela et al. 2012, 2017, 2018; Muñoz et al. 2019).

We performed a qualitative morphofunctional analysis of the extinct species analyzed, emphasizing the study of the features of joints with functional significance and the reconstruction of the muscles and their mechanical advantages. The known locomotor behaviors and substrate preferences of extant caviomorphs were used as a comparative model in the paleoecological analysis.

The study of the calcaneo-astragalar complex can reveal insights regarding the lifestyle of extinct rodents. Ginot et al. (2016) statistically showed and presented 15 measurements for the astragalus that are functionally related to rodent locomotory habits: astragalus body width (ABW), astragalus total length (ATL), astragalus total width (ATW), ectal facet length (EL), ectal facet width (EW), head height (HH), head width (HW), lateral body height (LBH), lateral trochlear length (LTL), medial body height (MBH), medial trochlear length (MTL), neck length (NL), sustentacular facet length (SL), sustentacular facet width (SW), trochlear width (TW) (Fig. 2 from Ginot et al. 2016). We used data from Ginot et al. (2016) for 35 extant species of Sciuromorpha, Supramyomorpha, and Hystricomorpha with known locomotor categories and replicated their linear discriminant analysis (LDA), adding *N. acreensis* (UFAC 1840 and UFAC 2549) a posteriori to compare their morphology with the extant species and assess the most probable locomotory habit of this species based on the astragalar morphology. In order to remove size differences among species, all linear measurements were log-transformed and divided by their geometric means, converting the linear measurements into log-shape ratios prior to LDA analysis (Claude 2008; Ginot et al. 2016). LDA was performed using the 'lda' function from MASS package in R (Venables and Ripley 2002). More details are available in Online Resource 1 and 2.

The plantar process of the navicular length/navicular body length index was calculated following Candela et al. (2017). The body mass of *Neoepiblema* was estimated by Kerber et al. (2017b) and Ferreira et al. (2020) based on cranial and dental dimensions (Millien 2008; Millien and Bovy 2010). To compare these results with the information from the postcranial bones, in this work, we also estimated the body mass using regression coefficients (ordinary least squares) of femoral and humeral measurements, which are based on several caviomorph taxa (Biknevicius et al. 1993). The diameters of the femoral and humeral shaft were taken at the positions corresponding to 65% and 35%, respectively, from the distal end of these bones. This approach was previously employed to estimate the body mass of *Phoberomys* (Sánchez–Villagra et al. 2003; Geiger et al. 2013). For comparison purposes, an additional approach was conducted to estimate body mass based on a volumetric rendering of *N. acreensis*. In order to obtain an anatomically plausible reconstruction of the animal (see below), a digital model was sculpted by paleoartist Márcio Castro, based on the known fossils of this rodent and observations of the general external morphology of extant chinchilloids. This approach emulates the volumetric assessments conducted by classical studies (e.g., Gregory 1905; Alexander 1985) based on physical sculptures (see Brassey 2017 for a review), and like those studies, it has some limitations. Most of these are due to the reliability of the skeletal reconstruction and the subjectivity induced by the interpretation of the soft tissue covering the bones. Given the inexistence of preserved bones of the thoracic region of *Neoepiblema*, a convex hull volumetric approach is unviable for the taxon, though other workers have successfully estimated plausible body mass values based on incomplete skeletons (e.g., Bates et al. 2015; Muller et al. 2020). Nonetheless, until more complete *N.*

acreensis skeletons are discovered, allowing assessment of the complete osteological proportions of this rodent, this remains the best way to perform a volumetric comparison with the estimates based on allometric equations. The volume of the model was calculated employing the free software Meshlab (Cignoni et al. 2008), and mass was then derived from the standard density equation, applying distinct mammal body densities compiled by Brassey and Sellers (2014).

The most informative bones were scanned using a laser scanner (Z–Scan 700) at the Centro de Apoio à Pesquisa Paleontológica/Universidade Federal de Santa Maria, and 3D models are available for download at morphomuseum.com (Kerber et al. 2021). The measurements were taken with digital calipers accurate to 0.01 mm, following Candela and Picasso (2008) and Ginot et al. (2016). The anatomical nomenclature primarily follows Candela and Picasso (2008), Wilson and Geiger (2015), and Candela et al. (2017). The employed myological nomenclature and the muscular system information was that of Woods (1972), McEvoy (1982), and García-Esponda and Candela (2010, 2016).

Analyzed Specimens

Neoepiblema acreensis

Niterói locality: **Humerus** – UFAC 3549, left humerus missing the proximal region. **Ulna** – UFAC 1939, right ulna missing the olecranon epiphysis and the distal region; UFAC 1940, right ulna missing the olecranon and the distal region; UFAC 2213, proximal region of a right ulna missing the olecranon; UFAC 2554, proximal region of a left ulna missing the olecranon. **Innominate** – UFAC 3697, right innominate bone; UFAC 2199, portion of a left innominate; UFAC 3666, portion of a left innominate. **Femur** – UFAC 2937, right femur with damaged proximal region; UFAC 4907, right femur missing the proximal and distal regions; UFAC 4882, proximal region of the diaphysis of left femur; UFAC 3698, right femur missing the proximal and distal regions; UFAC 2574, proximal region of a left femur; UFAC 4883, proximal region of left femur, with the proximal most region damaged; UFAC 2210, distal region of a right femur; UFAC 4808, distal region of a left femur; UFAC 2337, proximal region of a right femur. **Tibia** – UFAC 1887, right tibia; UFAC 2921, left tibia missing the proximal region; UFAC 2922, right tibia, missing the proximal region. **Astragalus** – UFAC 2549, right astragalus; UFAC 1840, left astragalus. **Metatarsal** – UFAC 2116, left metatarsal III; UFAC 3060, right metatarsal III. **Navicular** – UFAC 3672, right navicular.

Patos locality: **Humerus** – UFAC 5076, right humerus missing the proximal region.

Neoepiblema horridula

Talismã locality: **Humerus** – UFAC 4077, distal extremity of a right humerus; UFAC 2102, distal extremity of a left humerus. **Innominate** – UFAC 3260, fragmented left innominate; UFAC 3208, fragmented right innominate; UFAC 3207, fragmented left innominate; UFAC 3260, fragmented left innominate. **Femur** – UFAC 2737, proximal region of right femur; UFAC 3209, proximal region of left femur; UFAC 3210, proximal region of left femur; UFAC 2136, proximal region of a right femur; UFAC 2739, proximal region of right femur; UFAC 1698, proximal region of a right femur; UFAC 2620, distal region of a right femur. **Tibia** – UFAC 3202, right tibia, missing the proximalmost and distal portions; UFAC 2100, distal region of a right tibia. **Astragalus** – UFAC 3212, left astragalus.

Geological Settings

The fossils were found in outcrops (see above) of the Solimões Formation, Acre, Brazil. This sedimentary unit is exposed in the southwestern Brazilian Amazonia (states of Acre and Amazonas), mainly along the Acre, Juruá, and Purus rivers, and in road cuts (Cozzuol 2006; Negri et al. 2010; Ribeiro et al. 2013). In the upper levels of Solimões Formation, two main facies are recognized: a channel-dominated assemblage and a low-energy floodplain lacustrine assemblage (Latrubesse et al. 2007, 2010). The fossiliferous levels of the Solimões Formation were dated via U–Pb dating of detrital zircon, revealing ages between 10.89 ± 0.13 Ma (Talismã locality) and 8.5 ± 0.5 Ma (Niterói locality), Tortonian age (Bissaro-Júnior et al. 2019).

Availability of Data and Material

All data generated or analyzed during this study are included in this published article and its supplementary information files.

Institutional Abbreviations

CAPPA/UFSM-AC, comparative anatomy collection of the Centro de Apoio à Pesquisa Paleontológica da Quarta Colônia/Universidade Federal de Santa Maria, Brazil; **DGM**, paleontological collection of the Divisão de Geologia e Mineralogia, Museu de Ciências da Terra, Rio de Janeiro, Brazil; **MACN**, paleontological collection of the Museo Argentino de Ciencias Naturales "Bernardino Rivadavia", Buenos Aires, Argentina; **UFAC**, paleontological collection of the Universidade Federal do Acre (Campus Rio Branco), Rio Branco, Brazil; **UNEFM**, Universidad Nacional Experimental Francisco de Miranda, Coro, Venezuela.

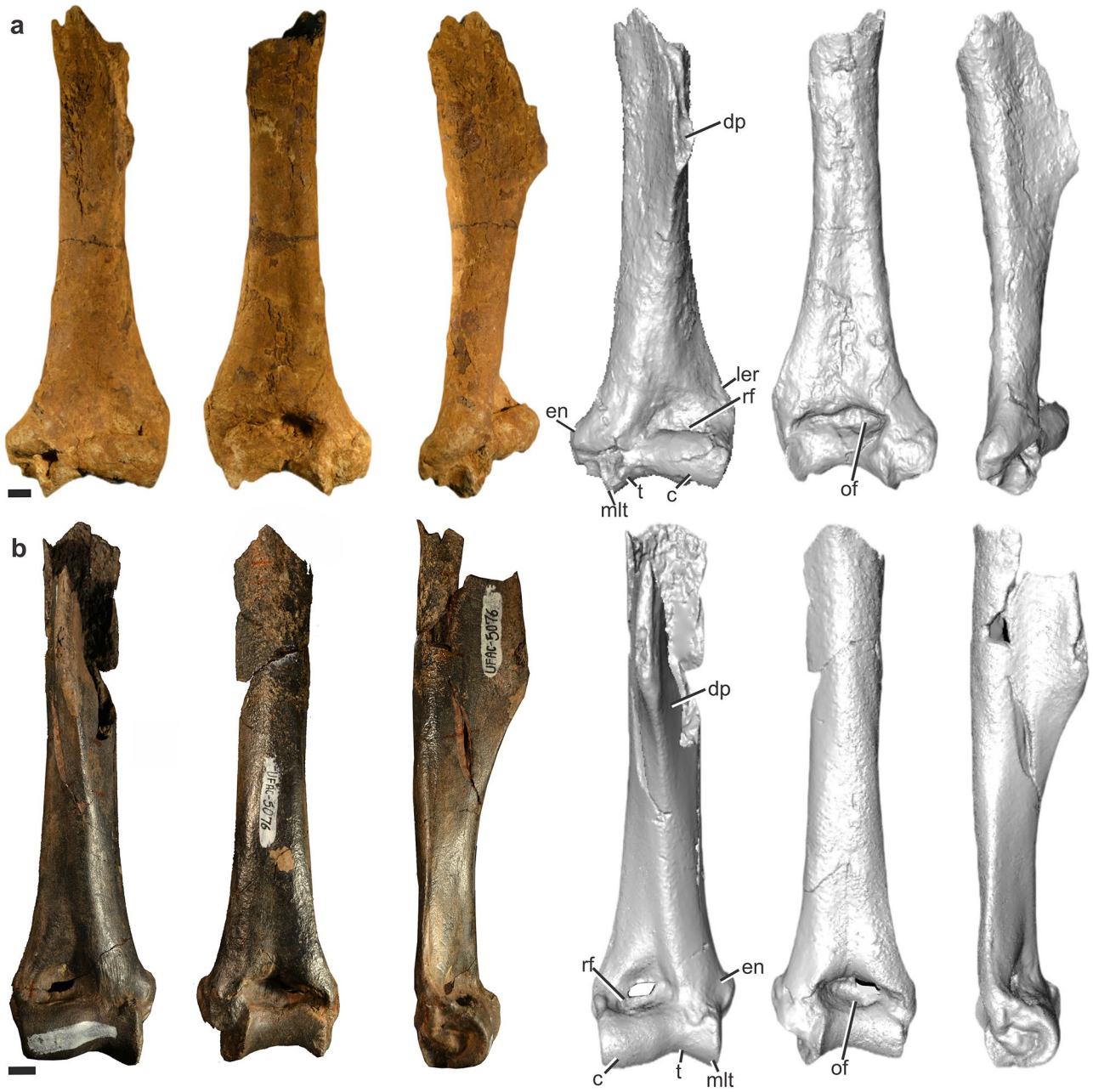

Fig. 2 Photographs (left) and three-dimensional model (right) of the humeri of *Neoepiblema acreensis*. **a**. UFAC 3549, left humerus, in cranial, caudal, and medial views; **b**. UFAC 5076, right humerus, in cranial, caudal, and lateral views. *Abbreviations*: *c*, capitulum; *dp*, deltopectoral crest; *en*, entepicondyle; *ler*, lateral epicondylar ridge; *mlt*, medial lip of the trochlea; *of*, olecranon fossa; *rf*, radial fossa; *t*, trochlea. Scale bars equal 10 mm

Table 1 Measurements (in mm) of the humerus of *Neoepiblema acreensis*

Measurement	UFAC 3549	UFAC 5076
Craniocaudal diameter	30.09	26.95
Transverse diameter	29.12	25.91
Transverse width	68.50	51.59
Distal articular surface width	53.95	41.58

Results

Comparative Morphology of Postcranial Bones of *Neoepiblema*

Humerus (Fig. 2, Table 1) None of the specimens preserves the proximal end of the humerus. The humeral shaft of *Neoepiblema* is columnar, not sigmoid as in *Phoberomys*

pattersoni (Fig. 2a, b), and its caudal face is flat. The deltopectoral crest is well developed and mediolaterally compressed (Fig. 2), distinct from *Dasyprocta*, *Cuniculus, Cavia,* and other cursorial rodents that have a weak crest. It is possible to observe that the deltopectoral crest of *Neoepiblema* extended from the proximal region down to the midportion of the diaphysis (Fig. 2), similar to *P. pattersoni* (Fig. 3a, b). However, in the latter, the deltopectoral crest is extended from the proximal region, distally surpassing the midportion of the diaphysis (Fig. 3a, b). In *Neoepiblema*

Fig. 3 Forelimb bones of *Phoberomys pattersoni* (UNEFM–F–020) from Urumaco Formation, Upper Miocene, Venezuela. **a–b**. right and left humeri, in craniomedial and caudolateral views. **c–d.** right and left ulnae, in cranial, medial, and lateral views. Scale bars equal 20 mm

and *P. pattersoni*, the crest is blade-shaped, and it does not taper cranially like that of extant chinchilloids (*D. branickii*, *L. maximus*, and *C. lanigera*) and *Perimys* (see Muñoz et al. 2019: fig. 2), in which this structure is well developed like a process, tapering cranially (character/state 9[1], Horovitz et al. 2006). The deltopectoral crest in *Neoepiblema* is slightly deflected laterally (Fig. 2), but less than in *Perimys*, *D. branickii,* and living erethizontids.

The radial fossa has a circular dorsal outline. It is shallow in UFAC 3549, but in UFAC 5076, it is deep like in *L. maximus*. There is no distinction between radial and coronoid fossae, as present in the Miocene erethizontid *Steiromys duplicatus*. The olecranon fossa is proximodistally short, moderately deep, and there is no supratrochlear foramen (Fig. 2), similar to *P. pattersoni* and *S. duplicatus* but distinct from *Perimys* and most extant caviomorphs in which a foramen is present or is intraspecifically variable (Horovitz et al. 2006).

At the distal articular surface, the epicondylar area is much less developed than that of *P. pattersoni*. In the latter taxon, the distal articular surface is transversely extended, much more than in *Neoepiblema*. The entepicondyle forms a robust tubercle, as in *D. branickii* and *L. maximus*, less developed than in *P. pattersoni.* This region of the humerus shows some variability in the analyzed specimens assigned to *Neoepiblema*. The entepicondyle of UFAC 3549 is more robust and medially more projected than in UFAC 5076. There is no entepicondylar foramen in the analyzed specimens, as present in Paleogene rodents (Rose and Chinnery 2004).

Table 2 Measurements (in mm) of the ulna of *Neoepiblema acreensis*

Measurement	UFAC 1939
Trochlea notch length	30.64
Olecranon process length	29.35
Proximal trochlea notch length	41.71
Olecranon coronoid process	55.51
Trochlear notch width	25.93
Transverse diameter	12.37

The capitulum is cylindrical and has a similar thickness along with its entire width (Fig. 2), being slightly shorter in UFAC 5076 than in UFAC 3549. In *L. maximus* and *D. branickii,* for example, the center of the capitulum is globose. There is no marked capitular tail and 'second trochlea' as present in *Perimys* and caviids (Muñoz et al. 2019). The medial lip of the trochlea is protruded distally, slightly surpassing the distalmost level of the capitulum.

The lateral epicondylar ridge of the humerus of *Neoepiblema* is moderately developed (more developed in UFAC 3549 than in UFAC 5076), similar to *D. branickii, L. maximus,* and *Phoberomys*, and distinct from caviids, in which the crest is poorly developed/absent, and from *S. duplicatus*, which shows a well-developed crest (Candela and Picasso 2008). Like the case of the deltopectoral crest, this region is more developed in *P. pattersoni*.

Ulna (Fig. 4, Table 2) The olecranon epiphysis of the analyzed specimens of *Neoepiblema* was not preserved because it was not fused in this ontogenetic stage (Fig. 4). A similar condition was recorded in *P. pattersoni* by Horovitz et al.

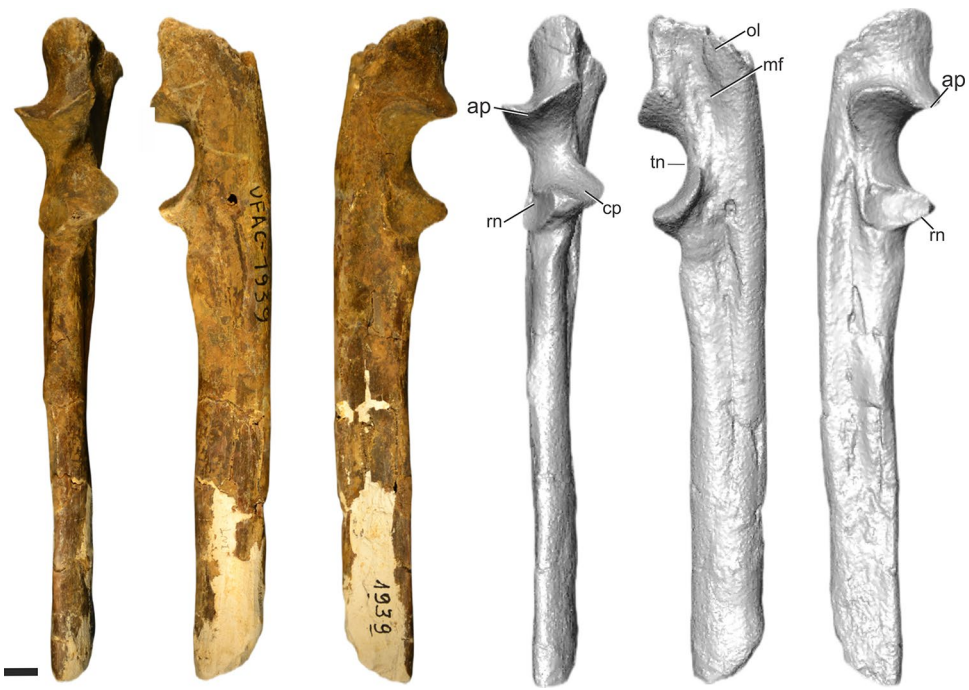

Fig. 4 Photograph (left) and three-dimensional model (right) of the right ulna (UFAC 1939) of *N. acreensis*, in cranial, medial, and lateral views. Abbreviations: *ap*, anconeal process; *cp*, coronoid process; *mf*, medial fossa; *rn*, radial notch; *tn*, trochlear notch; *ol*, olecranon. Scale bar equals 10 mm

(2006) (Fig. 3d). Both UFAC 1939 and the specimen described by Horovitz et al. (2006) have sizes compatible with adult individuals, suggesting that if the epiphysis fused, this would occur later in the ontogeny of neoepiblemids. Based on the preserved portion of the olecranon of the specimens assigned to *Neoepiblema*, it was proximally relatively well-developed (larger than the length of the trochlear notch), similar to *P. pattersoni* and *D. branickii*, but less proximally extended than *L. maximus.* It is oriented in line with the long axis of the ulnar shaft (8[1], Horovitz et al. 2006), like in *L. maximus*, and *Perimys* (Muñoz et al. 2019: fig. 4d), and not caudally oriented as in *Hydrochoerus hydrochaeris* (Fujiwara 2009; Candela et al. 2018). In *P. pattersoni*, it is slightly cranially oriented (8[0], Horovitz et al. 2006) in relation to the long axis (Fig. 3c-d). On the medial face of the olecranon, there is a fossa (medial fossa). On the cranial face, there is a proximodistally oriented ridge, which is not developed as in *L. maximus*. The ulnar shaft is relatively straight, and its thickness is uniform (Fig. 4) and distinct from *P. pattersoni*, in which it becomes thin distally (Fig. 3c-d). The ulnar shaft of *Perimys* is slightly curved craniocaudally, distinct from *Neoepiblema*, in which it is straight, and from *Phoberomys*, which shows a pronounced caudal convexity in the proximal segment of the diaphysis. In *L. maximus*, the shaft is slightly curved laterally and caudally. In *P. pattersoni* (Fig. 3a-b) and *D. branickii,* the distal region of the ulna is slightly curved (Horovitz et al. 2006: fig. 6). Along the ulnar shaft of *Neoepiblema*, there are shallow lateral and medial fossae. The trochlear notch, as usual, is concave, more than that of *Phoberomys* (Fig. 4). The anconeal process projects cranially to the same level as the coronoid process (Fig. 4). The radial notch is subrectangular, laterally positioned relative to the diaphyseal major axis (obliquely oriented), and craniocaudally concave. There is a single radial notch, differing from some cavioids such as *H. hydrochaeris*, in which this notch is composed of two separated facets for articulation with the radius (Candela et al. 2018). In *Neoepiblema* and *P. pattersoni*, the coronoid process is well developed with respect to the radial notch; it is transversely broad and cranially projected.

Table 3 Measurements (in mm) of the innominate of *Neoepiblema acreensis* (UFAC 3697) and *Neoepiblema horridula* (UFAC 3260)

Measurement	UFAC 3697	UFAC 3260
Acetabular length	37.92	28.75
Acetabular height	33.33	27.13

Innominate (Fig. 5, Table 3) The innominate bones here analyzed preserve portions of the ilium, ischium, and pubis (Fig. 5). Neither the main portion of the pubis nor the pelvic symphysis is preserved. In general, the innominate of *Neoepiblema* is quite similar to *P. pattersoni* and *L. maximus,* although there are some differences mentioned below. The ilium is craniocaudally elongated, in the same axis of the pubis, and its ventral outline is concave, as is the ventral surface of the pubis, which delimits the ventral edge of the obturator foramen. Judging by the preserved portion of this foramen (UFAC 3260), it is craniocaudally larger than in *D. branickii*, as it is in *P. pattersoni* and *L. maximus*. The acetabulum is a spherical cavity that appears to be proportionally greater in relative size in *Neoepiblema* than in *Phoberomys*. Inside it is located the acetabular notch, which is caudoventrally oriented and is broader than in *L. maximus*.

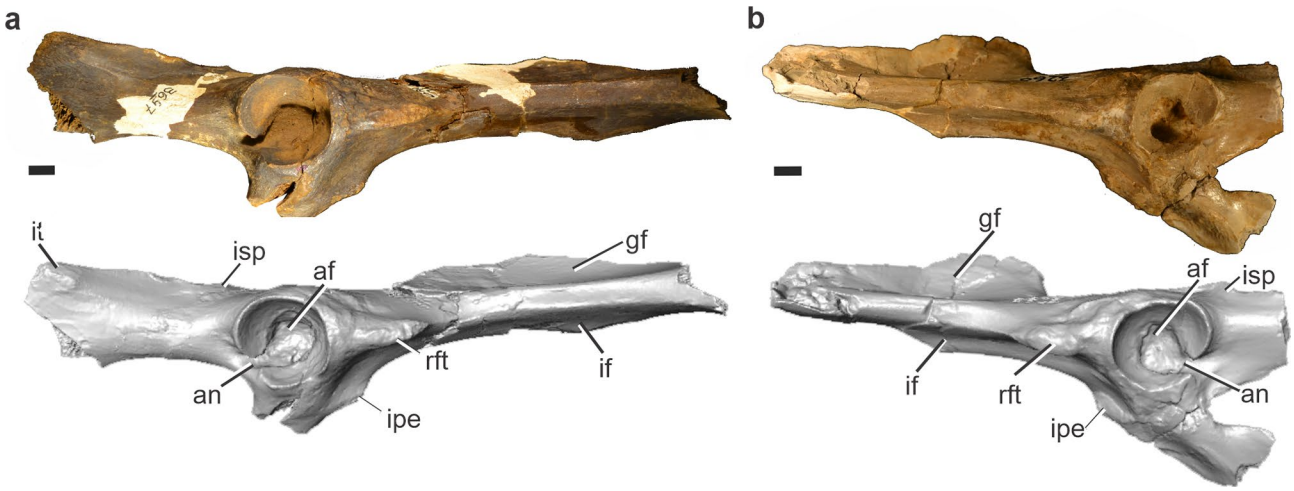

Fig. 5 Photographs (above) and three-dimensional models (below) of the innominate of *Neoepiblema acreensis* (**a**) and *Neoepiblema horridula* (**b**). **a**. UFAC 3697, right innominate, in lateral view; **b**. UFAC 3260, left innominate, in lateral view. *Abbreviations*: *af*, acetabular fossa; *an*, acetabular notch; *if*, iliac fossa; *ipe*, iliopubic eminence; *isp*, ischial spine; *it*, ischial tuberosity; *gf*, gluteal fossa; *rft*, rectus femoris tuberosity. Scale bars equal 10 mm

Fig. 6 Pelvic girdle and hindlimb bones of *Phoberomys pattersoni* (UNEFM-VF-020) from Urumaco Formation, Upper Miocene, Venezuela. **a**. left innominate, in lateral view; **b–c**. right and left femora, in cranial, caudal, and distal (right femur) views; **d**. right astragalus, in dorsal and ventral views; **e**. right navicular, in proximal and distal views. Scale bars equal 20 mm

The acetabular notch is connected to the acetabular fossa, which is rounded (Fig. 5). The cranial edge of the acetabulum projects more laterally than the dorsal, ventral, and caudal edges.

On the lateral surface of the ilium, cranial to the acetabulum, there is a robust tuberosity for the *m. rectus femoris* (Fig. 5). Dorsocaudally to the acetabulum, there is a weak ischial spine. The gluteal fossa is broader and deeper than the iliac fossa. In UFAC 3260, the gluteal fossa is more concave than in UFAC 3697. Cranioventral to the acetabulum, there is a marked iliopubic eminence, as in *L. maximus* and *P. pattersoni* (Fig. 6a), which is not evident in some caviomorphs, such as *H. hydrochaeris*.

Based on the preserved portion of the ischium of specimen UFAC 3697, it appears to be proportionally slenderer than in *P. pattersoni*. On its caudal region, a portion of the ischial tuberosity is preserved, and this one seems to be less robust than in *P. pattersoni*, in which this structure is dorsally projected (Fig. 6a).

Femur (Figs. 7, 8 and Table 4) The femoral neck and head are slightly cranially oriented in relation to the long axis of the femur (Fig. 7b). The femoral head is spherical, like in most living rodents (Figs. 7a, b, Fig. 8a). The fovea capitis femoris is medially positioned, and it is caudally oriented. The greater trochanter is tall, surpassing the head of the femur (Figs. 7a, b, 8a), similar to *Phoberomys* (Figs. 6b, c, 9, 10), *L. maximus*, and distinct from *D. branickii*, in which the greater trochanter is only slightly taller than the femoral head. In some rodents, such as erethizontids and *Cavia*, the proximalmost area of the greater trochanter is at the same level as the femoral head. This trochanter protrudes laterally beyond the shaft of the femur, such as in *Phoberomys, H. hydrochaeris*, *Dolichotis*, and chinchillids. In *L. maximus*, there is an isolated protuberance on this lateral projection of the greater trochanter, which is not present in *N. acreensis* (Fig. 7a, b) or *Phoberomys* (Figs. 6b, c, 9, 10) but is present in a femur assigned to *N. horridula* (UFAC 2737) (Fig. 8a). It is important to note that in *D. branickii*, the greater trochanter does not protrude laterally. In UFAC 2574, the epiphyseal line of the greater trochanter is visible (Fig. 7b). In *N. acreensis* (UFAC 2937 and UFAC 2574) as well as in *N. horridula* (UFAC 2620), there is a longitudinal depression on the lateral surface of the femur, at the level of the lesser trochanter (Figs. 7a, b, 8a), which is also present in some caviomorphs, such as *D. branickii* and *L. maximus*. The lesser trochanter forms a rounded tuberosity on the caudal face of the femur, slightly medially oriented (caudomedially), similar to *D. branickii* and not medially extending as in *C. lanigera* and *L. maximus*, in which this protruding structure can be observed in cranial view. In *Phoberomys*, the lesser trochanter is oriented more medially than in *Neoepiblema*, but not as in chinchillids. As also occurs in *Phoberomys*, the intertrochanteric crest is not connected to the lesser trochanter.

The femoral diaphysis of *Neoepiblema* (Fig. 7a, b) is straight and increases in thickness distally. It is slenderer than that of *Phoberomys* (Figs. 6b, c, 9, 10). In *Phoberomys* sp. (DGM 601-M), the diaphysis is laterally curved (Fig. 10), but not in *P. pattersoni* (Fig. 6b, c), nor in femora assigned to *P. burmeisteri* (Fig. 9), indicating differences between the Solimões Formation specimen and other specimens.

There is no third trochanter in the femur of *Neoepiblema*, different from the condition found in some caviomorphs (e.g., *Cuniculus*, *Dasyprocta*, *D. branickii*; Mones 1997; Wilson and Geiger 2015). In the right femur of *P. pattersoni* (UNEFM-VF-020), there is a small tuberosity located laterally (Fig. 6b), slightly distal to the midpoint of the diaphysis, that could correspond to the third trochanter.

On the distal region of the femur (Fig. 7a, c, d), the patellar ridges are almost parallel but slightly convergent proximally. As in *Phoberomys* (Figs. 6b, c, 9, 10), *C. lanigera,* and *L. maximus*, the medial ridge is more elevated than the lateral one, which is distinct from the pattern observed in *D. branickii* (Mones 1997, fig. 9c), *Coendou*, and *Cavia* (Candela and Picasso 2008: fig. 13), in which both ridges are at the same level, or the lateral is slightly raised with respect to the medial one (Horovitz et al. 2006). The lateral and medial femoral condyles diverge laterally and medially, respectively. In distal view, the medial condyle is slightly wider than the lateral one, as is true of the neoepiblemid from the Ituzaingó Formation assigned to *P. burmeisteri* (MACN 3147). In *D. branickii* they are subequal, and in *L. maximus* and *Phoberomys* sp. (DGM 601-M), the lateral condyle is somewhat wider.

In distal view, the epiphysis of the femur shows the transverse diameter equivalent to or slightly larger than the craniocaudal diameter (Figs. 7d, 8c), similar to *L. maximus*, *C. lanigera*, erethizontids, and distinct from cursorial caviids that show the opposite (Candela and Picasso 2008). Specimens assigned to *Phoberomys* from Argentina and Brazil (Figs. 9, 10) show the same pattern as in *Neoepiblema*, as does UNEFM–VF–020 (*P. pattersoni*) from Venezuela (Fig. 6 d). However, it is not possible to analyze this trait precisely in UNEFM–VF–020 because the femora are taphonomically compressed.

Tibia (Fig. 11, Table 5) The tibia of *Neoepiblema* is quite similar to *L. maximus*. No specimen preserves the proximal epiphysis, and for this reason, the morphology of the condyles is unknown. In cranial view, the tibia is straight, and in lateral view, it is slightly curved cranially (Fig. 11). On the cranial face of the tibia, the tibial (=cnemial) crest is well marked and slightly deflected laterally. It is not so cranially projected as in erethizontids, but it is distally extended, almost reaching the middle of the diaphysis. On the lateral aspect of the tibia, the popliteal line is visible in both analyzed specimens of *Neoepiblema acreensis* (UFAC 1887) and *N. horridula* (UFAC 3202). The lateral fossa is relatively well-developed.

On the distal end of the tibia, the most salient feature is the distal tibial spine, which is located cranially to the lateral astragalotibial trochlea facet (Fig. 11). Medially to this spine, there is another spine, reduced in comparison, positioned cranial to the medial astragalotibial trochlea facet. The posterior process is located on the caudal region of the distal end of the tibia. It is poorly developed and has a hooked shape. On the caudal surface of the posterior process lies the groove for the tendon of the *m. flexor digitorum fibularis*, which is proximodistally oriented (Fig. 11). As described for *Phoberomys pattersoni*, the medial malleo-

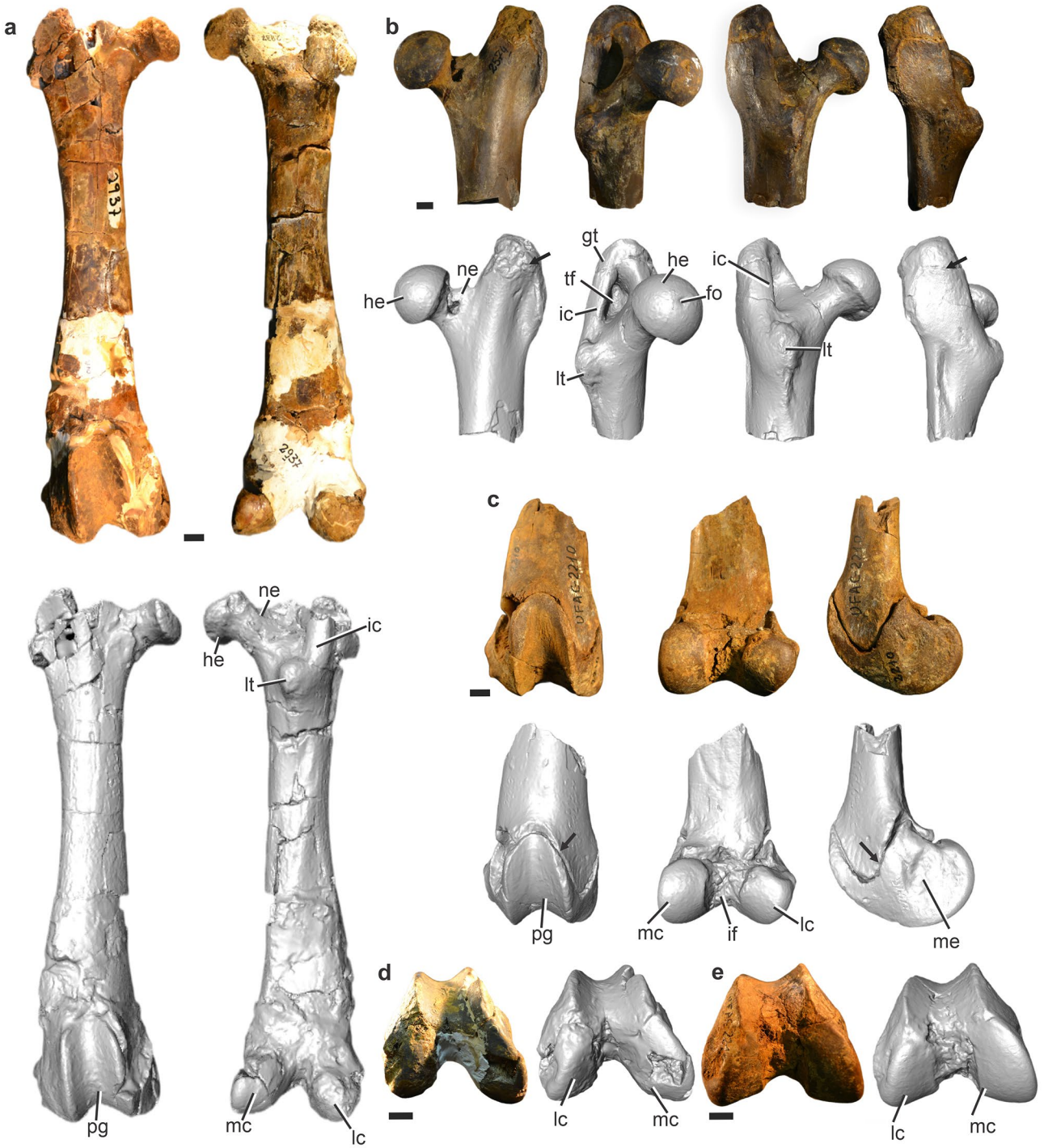

Fig. 7 Photographs and three-dimensional models of the femora of *Neoepiblema acreensis*. **a**. UFAC 2937, right femur, in cranial and caudal views; **b**. UFAC 2574, proximal portion of left femur, in cranial, mediocaudal, caudal, and lateral views; **c**. UFAC 2210, distal portion of right femur in cranial, caudal, and medial views; **d–e.** distal views of the specimens UFAC 2937 (**d**) and UFAC 2574 (**e**). *Abbreviations*: *ic*, intertrochanteric crest; *if*, intercondylar fossa; *fo*, fovea capitis femoris; *gt*, greater trochanter; *he*, head; *lc*, lateral condyle; *lt*, lesser trochanter; *mc*, medial condyle; *me*, medial epicondyle; *ne*, neck; *pg*, patellar groove; *tf*, trochanteric fossa. Arrows indicate the epiphyseal lines. Scale bars equal 10 mm

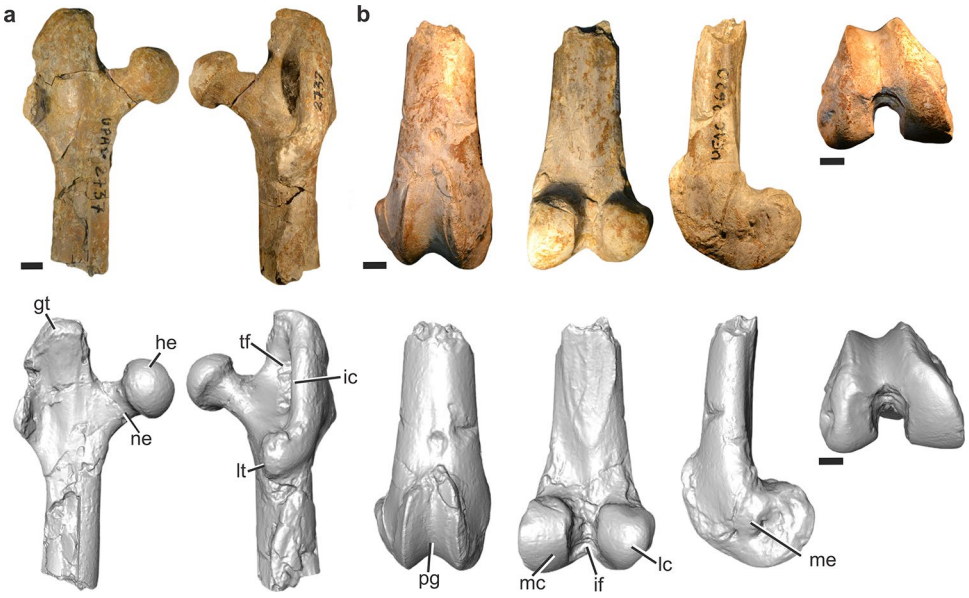

Fig. 8 Photographs (above) and three-dimensional models (below) of the femora of *Neoepiblema horridula*. **a**. UFAC 2737, proximal portion of right femur in cranial and caudal views; **b.** UFAC 2620, distal portion of right femur in cranial, caudal, medial, and distal views. *Abbreviations*: *ic*, intertrochanteric crest; *if*, intercondylar fossa; *gt*, greater trochanter; *he*, head; *lc*, lateral condyle; *lt*, lesser trochanter; *mc*, medial condyle; *me*, medial epicondyle; *ne*, neck; *pg*, patellar groove; *tf*, trochanteric fossa. Scale bars equal 10 mm

lus is poorly developed. Caudal to the latter structure is the groove for the tendon of the *m. flexor digitorum tibialis* + *m. tibialis caudalis.* The medial and lateral astragalotibial facets are concave and separated by a prominent lateromedially oriented ridge. The lateral facet is wider than its medial counterpart.

Astragalus (Fig. 12, Table 6) The astragalar neck is relatively short (shorter than in *L. maximus*). The astragalar head projects slightly craniomedially in relation to the medial tibial ridge (Fig. 12) (similar to *L. maximus* and *D. branickii*), being oriented less medially than in erethizontids and *P. pattersoni* (Fig. 6d) and not as cranially as in *Dolichotis* and *Cavia* (Candela and Picasso 2008: fig. 19), in which the astragalar neck and head are predominately cranially oriented. The astragalar head is transversally wider than in *L. maximus*, *C. lanigera*, and *D. branickii* and not as rounded as in erethizontids. In *N. horridula*, the astragalar head is transversally narrower than in *N. acreensis*. The navicular facet is dorsoplantarly convex and transversely wide. In dorsal view, there is a transverse sulcus on the neck (Fig. 12).

On the trochlea, the medial ridge is narrower and projects slightly more caudally than the lateral ridge, and the slope of the lateral tibial ridge is less pronounced than that of the medial ridge. A medial ridge projected more caudally than the lateral is shared with *P. pattersoni* and *D. branickii* and, according to Horovitz et al. (2006), this is a different pattern from the condition found in *L. maximus*, *C. lanigera*, and *H. hydrochaeris,* for instance, where both ridges are subequal. Also, the astragalar features of *Neoepiblema* are slightly different from *P. pattersoni* because trochlear ridges of the former are less developed and the groove between them is shallower.

In plantar view, the ectal and sustentacular facets are separated by a deep astragalar sulcus (Fig. 12). There is a shallower groove separating the sustentacular facet from the astragalomediotarsal facet. This groove ends at the navicular facet. The sustentacular facet is pyriform,

Table 4 Measurements (in mm) of the femur of *Neoepiblema acreensis* (UFAC 2937, UFAC 2210, UFAC 2574) and *Neoepiblema horridula* (UFAC 2737, UFAC 2620)

Measurement	UFAC 2937	UFAC 2210	UFAC 2574	UFAC 2737	UFAC 2620
Functional length	242.86	–	–	–	–
Head length	–	–	32.70	25.80	–
Head width	–	–	32.13	26.31	–
Transverse diameter at mid-shaft	30.83	–	–	26.87	–
Distal depth	64.38	61.99	–	–	53.09
Distal end width	65.27	64.92	–	–	53.52
Medial condyle width	24.70	22.86	–	–	19.52
Lateral condyle width	22.45	21.70	–	–	21.95

Fig. 9 Neoepiblemid femora from Ituzaingó Formation (Upper Miocene), Argentina. **a.** proximal region of the femur of *Phoberomys burmeisteri* (MACN 3344) described by the Argentinean paleontologist Lucas Kraglievich (1932), in cranial and caudal views; **b.** right neopiblemid femur (MACN 3147), in cranial, caudal, and distal views. Scale bars equal 20 mm

craniocaudally oriented, and cranially wider than its caudal portion. Cranially, it is convex and contacts the navicular facet, and caudally it is slightly concave and separated from the medial ridge by a shallow sulcus (Fig. 12). In *C. lanigera*, this sulcus is wider than in *Neoepiblema* and *L. maximus*. Medially, the astragalomediotarsal facet of the astragalar head (for the medial tarsal bone) is rounded and is well developed. Cranially, it is continuous with the navicular facet. The ectal facet is concave and opposed to the lateral ridge. It is wider than the sustentacular facet, and its caudal portion is wider than the cranial part.

The transverse diameter of the astragalus of *N. acreensis* is slightly larger than the proximodistal length (in *N. horridula,* the transverse diameter is slightly shorter than the proximodistal length), similar to erethizontids, *D. branickii,* and *P. pattersoni*. In extant chinchillids, as well as in caviids, the astragalar body is markedly narrower (transverse diameter shorter than the proximodistal length).

Navicular (Fig. 13, Table 7) The facet for the astragalar head on the navicular body (UFAC 3672) has well-delimited margins (Fig. 13a), as in *P. pattersoni* (Fig. 6e). This facet is oval (Fig. 13a), and the transverse diameter is larger than the dorsoplantar one. In the plantar aspect, there is a notch on the ventral margin of the facet. The ectocuneiform facet is located on the distal face and has a subtriangular outline. This face is slightly concave (Fig. 13a). Lateral to the ectocuneiform facet is located the cuboid facet, which is flat and larger than either cuneiform facet. Medial to the ectocuneiform facet, there is a dorsoplantarly elongated and lateromedially narrow facet for the mesocuneiform. On the medial surface of the navicular, there are two facets. The first one is dorsally located, forming a prominence, possibly for the articulation with the medial tarsal bone. The second one is located on the plantar surface (almost on the medial surface of the plantar process), possibly for the entocuneiform. Plantar to the navicular body, there is a robust, but relatively short, plantar process (Fig. 13a, b). The plantar face of this structure is inclined medially.

Metatarsal III (Fig. 14, Table 8) The metatarsal III (UFAC 2116) lacks the distal epiphysis, which was not fused to the shaft at the time of fossilization (Fig. 13c). It is relatively short, not elongated as in *Chinchilla* and *Lagidium* (Candela et al. 2017, fig. 4). The shaft is dorsoplantarly curved and compressed (Fig. 13c). The proximal surface (ectocuneiform facet) is flat and oblique (medially inclined) (Fig. 12c). This facet has a subtriangular plantar prolongation. The metatarsal II facet is located proximolaterally, forming a shallow concavity (Fig. 13c).

Astragalar Morphometrics

The first two LDA axes summarized 71.61% of astragalus morphological variation. LD1 (46.76%) is positively

Fig. 10 Left femur of *Phoberomys* sp. (DGM 601-M) from Solimões Formation (Upper Miocene), Brazil, described by the Brazilian paleontologist Carlos de Paula Couto (1978). In cranial, caudal, medial, lateral, and distal views. Scale bars equal 20 mm

correlated with ATW, NL, SW, and TW and negatively correlated with LBH, MBH, MTL, and SL, separating arboreal climbers and fossorial/semi-fossorial species (positive scores) from the other locomotory habit types (intermediate scores) and the jumping locomotor habit (lowest scores) (Table 9, Fig. 14). LD2 (24.85%) is positively correlated with HH, while negatively correlated with ABW and MBH (Table 9; Fig. 14). It separates species with jumping and arboreal-climbing habits (positive scores) from the other habit types (negative scores). Extreme negative scores converging at both LD1 and LD2 (lower left region of the plot) represent cursorial and terrestrial generalist species, with *Neoepiblema acreensis* being positioned adjacent to these two habits, with a probability of 0.838 of correct classification within the cursorial habit (Fig. 14).

Body Mass Estimates

The body mass of *Neoepiblema acreensis* and *N. horridula* was estimated based on the diameter of the long bones here described, using the equations of Biknevicius et al. (1993) (Table 10), which resulted in 158.95 kg (average) for *N. acreensis* and 63.44 kg for *N. horridula*. A second analysis employed a volumetric study of the digital sculpture of *N. acreensis* (Fig. 15). The digital sculpture was rescaled to fit the total size of the skull UFAC 4515, resulting in a model with 140 cm in total body length, 57.8 cm in height, and a body volume of 0.073m^3. These body volumes were applied to different body densities obtained from the literature and measured for different animals with differing methods (Brassey and Sellers 2014). The resulting body mass estimates range from 65.3 –77.2 kg for *N. acreensis* (Table 11).

Discussion

Functional Morphology of the Postcranial Bones of *Neoepiblema* and Paleobiological Implications

Forelimb The proximal region of the humerus is not preserved in any analyzed specimen assigned to *Neoepiblema*. This region provides important information about the functional aspects of the forelimbs of rodents (Candela and Picasso 2008). Among neopiblemids, in *Phoberomys pattersoni*, as in *Perimys*, the humeral tuberosities are slightly lower than the proximal end of the humeral head. This may allow movement at the glenohumeral joint level, as has been suggested in previous studies (Argot 2001; Sargis 2002a;

Candela and Picasso 2008; Muñoz et al. 2019). However, as was indicated by Muñoz et al. (2019), it is not possible to associate this trait with a particular type of substrate use. Low humeral tuberosities are present in forms with different substrate uses, such as *Myocastor* (swimmer and digger) and *Ctenomys* (digger). In the case of *Phoberomys,* it is possible to infer that the glenohumeral joint was not restricted to parasagittal movements, permitting some degree of mobility. Despite its incompleteness, some humeral traits with functional relevance are present in the *Neoepiblema* specimens presented here. The deltopectoral crest is well-developed and cranially projected, which indicates that muscles related to adduction and internal rotation (*m. clavodeltoideus*), extension and abduction (*m. acromiodeltoideus*), flexion and external rotation (*m. spinodeltoideus*), and adduction-protraction of the humerus (*m. pectoralis*) were powerful. This is advantageous for various activities, such as running, climbing, swimming, and digging (Candela and Picasso 2008; Candela et al. 2012; Muñoz et al. 2019). The distally extended deltopectoral crest present in *Neoepiblema* increases the mechanical advantage of both muscle groups, deltoid and pectoral. In *Phoberomys*, the greater distal extension of the deltopectoral crest indicates a greater mechanical advantage for the action of these muscles than in *Neoepiblema*. In *Neoepiblema*, this crest is slightly deflected laterally, indicating a craniolateral protrusion of this structure, similar to that of *Perimys* but to a lesser degree. According to Muñoz et al. (2019), the craniolateral protrusion of the deltopectoral crest could be associated with a greater mechanical advantage for external rotation of the humerus by *m. spinodeltoideus* relative to *m. pectoralis major*, which could be related to lateral movement of the forearm. This trait also appears in *Ctenomys* and *L. maximus* (diggers) and *M. coypus* (digger and swimmer) (Muñoz et al. 2019), suggesting a mechanical advantage of this condition for such habits. In the case of *Perimys*, Muñoz et al. (2019) suggested that it could be used when extracting sediment when digging.

The lateral epicondylar ridge is the area of origin of the extensors of the manus (*m. extensor carpi radialis*). In addition, this crest offers the surfaces of attachment for the *m. triceps brachii caput lateralis* and *m. anconeus* posteriorly. This region is moderately developed in *Neoepiblema*. Like the case of the deltopectoral crest, this region is more prominent in *P. pattersoni*, indicating important musculature related to the extension of the forearm (Candela and Picasso 2008). The broad insertion area inferred for the *m. anconeus* in *P. pattersoni* could contribute to the stabilization of the elbow joint (Argot 2001), which would be advantageous in strengthening this joint to withstand the large loads associated with its large body size. The entepicondyle is the attachment site of the *m. pronator teres* and the flexor muscles of the manus (McEvoy 1982; Argot 2001). *Neoepiblema* shows a robust entepicondyle, as in *D. branickii* (Mones 1997), *L. maximus*, and *C. lanigera* (Candela and Picasso 2008), which is even greater in *P. pattersoni,* distinct from cursorial caviids, in which this structure is reduced. The great development of the entepicondyle could be related to the mechanical advantage of the muscles involved in the flexion of the hand and digits. The powerful flexion of the hand is important in the ability to grasp, dig and/or manipulate food and is also compatible with swimming (Taylor 1974; Argot 2001; Sargis 2002a; Samuels and Van Valkenburgh 2008; Muñoz et al. 2019). The use of the forelimb to manipulate food in neoepiblemids was inferred by Sánchez-Villagra et al. (2003), based on the disparity in size of fore- and hindlimbs of *P. pattersoni*. The lateromedially expanded distal articular surface of the humerus in *P. pattersoni* could indicate a greater resistance to the large forces generated at the level of the elbow joint to support the great weight (body size) of this species. Additionally, it is associated with powerful hand flexion (Elissamburu and Vizcaíno 2004).

The olecranon fossa is moderately deep and not perforated (broken in UFAC 5076). The depth of this fossa is quite variable in caviomorphs, and the presence/absence of a perforation in this fossa is also variable (Horovitz et al. 2006). The olecranon fossa is shallow and not perforated in extinct erethizontids, which do not have a full elbow extension (Candela and Picasso 2008; Candela et al. 2012). On the other hand, other caviomorphs that present a deep and perforated olecranon fossa have an increased extension of the antebrachium and more stabilized craniocaudal movement of this region of the forelimb because the anconeal process traverses this fossa during complete extension (Candela and Picasso 2008; Candela et al. 2012, 2018; Muñoz et al. 2019). As mentioned before, in *Neoepiblema* and *Phoberomys*, the fossa is moderately deep and not perforated. Therefore, the full extension of the forearm would not have been possible, as occurs in the capybara, for example, in which the olecranon fossa is deep and perforated. In this sense, *Neoepiblema* could have had incomplete forelimb extension, limited stability, and restricted range of movement during extension, as well as a frequently semi-flexed posture. However, the olecranon fossa is deeper than in erethizontids, permitting greater extension than in porcupines (Candela and Picasso 2008; Candela et al. 2018), compatible with ambulatory habits.

Neoepiblema does not show a developed humeral capitular tail and 'second trochlea', which are evident in caviids (Muñoz et al. 2019). The presence of such traits maximizes the stability at the humeroradial joint because they limit the movement of the forearm to the sagittal plane (Candela et al. 2012, 2018; Muñoz et al. 2019). Conversely, their absence facilitates pronation and supination movements (Candela and Picasso 2008). Notwithstanding, *Neoepiblema* shows a cylindrical capitulum, which is more restrictive concerning


a
b
tc
tc
pl
dts
c
dts
mm
matf
latf
gfdf
mm
gfdt
gfdf
mm
dts
pp

◂**Fig. 11** Photographs (above) and three-dimensional models (below) of the tibia of *Neoepiblema acreensis* (**a, c**) and *Neoepiblema horridula* (**b**). **a.** UFAC 1887, right tibia in cranial, medial, and lateral views; **b.** UFAC 3202, right tibia in cranial, medial, and lateral views; **c.** distal region of UFAC 1887, in cranial, distal, and caudal views. *Abbreviations*: *dts*, distal tibial spine; *gfdf*, groove for tendon of *m. flexor digitorum fibularis*; *gfdt*, groove for tendon of *m. flexor digitorum tibialis* + *m. tibialis caudalis*; *latf*, lateral astragalotibial trochlea facet; *matf*, medial astragalotibial trochlea facet; *mm*, medial malleolus; *pl*, popliteal line; *pp*, posterior process; *tc*, tibial crest. Scale bars equal 10 mm

pronation and supination movements than in forms with a rounded capitulum, such as extant erethizontids (Candela and Picasso 2008; Candela et al. 2012). Hence, according to the traits observed in *Neoepiblema*, it is suggested that the elbow joint allowed a certain degree of supination, although not to the degree observed in climbing forms, since some traits indicate a certain amount of stability (medial lip of the protruding trochlea, cylindrical capitulum). Inferred pronation and supination movements are compatible with food manipulation.

Concerning the ulnar morphology, the analyzed specimens do not preserve the epiphyses, which were not fused at the time of death. Nevertheless, judging by the preserved portion, it was likely relatively well-developed (see description). The longer the olecranon, the greater the out-lever arm of the *m. triceps brachii*, which is of adaptative value to dig or swim (Hildebrand 1974; Van Valkenburgh 1987; Vizcaíno et al. 1999; Argot 2001; Candela and Picasso 2008; Samuels and Van Valkenburgh 2008; Candela et al. 2012, 2018). This structure is elongate and not caudally oriented, as in the capybara *H. hydrochaeris* (Fujiwara 2009; Candela et al. 2018). According to previous interpretations of the caviomorph elbow joint (Candela et al. 2018), *Neoepiblema* would have had a more crouched forelimb than *H. hydrochaeris*. In forms with a straight olecranon (proximally oriented in relation to the long axis of the ulnar shaft) or cranially bent, the triceps leverage is maximized when the elbow is relatively flexed. On the other hand, when the olecranon is caudally oriented, as in the capybara, the triceps leverage is maximized with a more extended elbow (Van Valkenburgh 1987). The proximal ulnar region of *P. pattersoni* and *D. branickii* is more cranially bent than in *Neoepiblema*. In this sense, *Neoepiblema* would have had a less crouched forelimb than those rodents. As in arboreal erethizontids, in *Phoberomys*, the convexity of the caudal border of the ulna could be related to the combination of the great efforts produced by the flexor and extensor muscles, in association with the large body size of this rodent.

The single radial notch is distinct from the pattern found *H. hydrochaeris,* in which the notch has two facets (Candela et al. 2018). Additionally, the radial notch is more laterally positioned than in caviids and *Perimys*, in which this structure is more cranially located because the head of the radius occupies a more cranial position in the antebrachium and has restricted supination movements (Candela et al. 2018). Judging by the position of the radial notch and the great development of the coronoid process, it can be inferred that during locomotion the forces (weight support) between the radius and ulna at the elbow joint would have been equivalently distributed. The laterally positioned and concave radial notch would allow rotational movements of the radius compatible with food manipulation.

Pelvic girdle The innominate bone shows a well-developed rectus femoris tuberosity. In this tuberosity originates part of the *m. quadriceps femoris* group, which is a flexor of the hip and extensor of the knee. Its strong development is associated with a powerful flexion of the hip and extension of the knee, as it occurs in forms with strong propulsion of the limb.

The wide gluteal fossa for the origin of the *m. gluteus medius* and *m. gluteus profundus*, indicates that these muscles were well developed and thus provided a powerful extension of the hip. A wide gluteal fossa is present in species with diverse substrate uses, such as runners and diggers. A well-developed iliac fossa, which provides the origin area for the *m. iliacus*, is compatible with a powerful flexion of the hip joint when the leg is fixed in position. A relatively powerful flexion of the hip would provide an advantage to resist the forces generated during digging and to anchor the body firmly in the substrate but also to resist the large forces during locomotion and maintenance of posture in association with the large body size of these rodents. The robust ischial tuberosity (especially in *P. pattersoni*) for the origin of the hamstring muscles (*m. biceps femoris* and *m. semitendinosus*) indicates a strong development of these muscles, compatible with a strong extension of the hip and flexion of the knee. The greater development of this tuberosity in *Phoberomys* indicates a stronger development of hamstring muscles, probably in relation to its large body size, compatible with strong propulsion of the leg at the beginning of the propulsive stroke.

Hindlimb The femur shows a well-developed greater trochanter, projecting further proximally than the femoral head and extending laterally, as in *Phoberomys* (Horovitz et al. 2006). This structure is the attachment site for the *m. gluteus medius* and *m. gluteus profundus*, which act as extensor/abductor muscles of the hip (Maynard Smith and Savage 1956; McEvoy 1982; García Esponda and Candela 2016). A well-developed greater trochanter (proximally and laterally) indicates the presence of a powerful thigh musculature, used during propulsion (Maynard Smith and Savage 1956; Argot 2002; García-Esponda and Candela 2010), as is common in cursorial and saltatorial forms but not in arboreal caviomorphs (Candela and Picasso 2008). According to Candela and Picasso (2008), the proximal development of

Table 5 Measurements (in mm) of the tibia of *Neoepiblema acreensis* (UFAC 1887) and *Neoepiblema horridula* (UFAC 3202)

Measurement	UFAC 1887	UFAC 3202
Length	252.45	–
Tibial crest length	125.10	77.80
Proximal end width	49.60	33.12
Proximal end length	–	33.18

the greater trochanter also restricts femoral mobility during abduction movements, which are important for climbing in erethizontids. Note that the chinchilloid *D. branickii* shows a pattern different from that observed in *Neoepiblema*, *P. pattersoni*, and chinchillids, in which the greater trochanter slightly surpasses the femoral head but is not laterally projected. This pattern is consistent with the scansorial habits of the species (Wilson and Geiger 2015), which can walk on an irregular substrate, climbing fallen logs and rocks, situations in which the abduction movement is important.

The lesser trochanter is the attachment site of the *m. iliopsoas* (*m. iliacus* + *m. psoas major*) (McEvoy 1982; García-Esponda and Candela 2010), a flexor of the hip joint. In *Neoepiblema* and terrestrial caviomorphs, the trochanter is caudomedially oriented, while in *L. maximus* and *C. lanigera*, it is medially protruding, reaching the maximum medial expansion in erethizontids (Candela and Picasso 2008). Muñoz (2021) indicated that a medially projected lesser trochanter is present in climber/digger/swimmer mammals. The iliopsoas muscle complex of animals with a medially protruding lesser trochanter would be advantageous to externally rotate the femur during the locomotion, differing from animals in which this structure is caudally oriented, favoring parasagittal

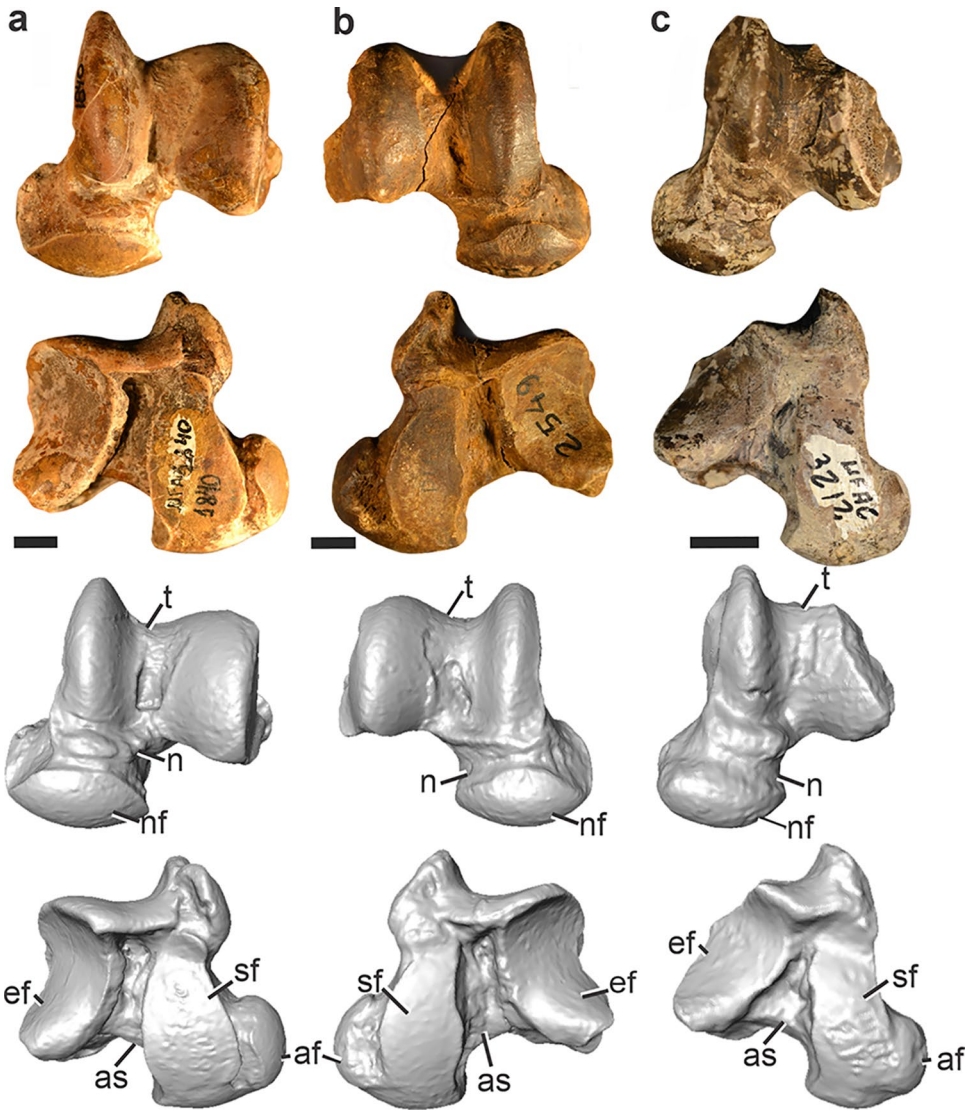

Fig. 12 Photographs (above) and three-dimensional models (below) of the astragali of *Neoepiblema acreensis* (**a–b**) and *Neoepiblema horridula* (**c**). **a.** UFAC 1840, left astragalus, in dorsal and plantar views; **b.** UFAC 2549, right astragalus, in dorsal and plantar views; **c.** UFAC 3212, left astragalus, in dorsal and plantar views. *Abbreviations*: *af*, astragalomediotarsal facet; *as*, astragalar sulcus; *ef*, ectal facet; *n*, neck; *nf*, navicular facet; *sf*, sustentacular facet; *t*, trochlea. Scale bars equal 10 mm

Table 6 Measurements (in mm) of the astragalus of *Neoepiblema acreensis* (UFAC 2549, UFAC 1840) and *Neoepiblema horridula* (UFAC 3212)

Measurement	UFAC 2549	UFAC 1840	UFAC 3212
Body width	46.05	51.86	32.90
Medial tarsal facet length	20.61	23.01	11.33
Total length	54.53	57.02	38.33
Total width	56.09	58.17	35.24
Ectal facet length	26.90	30.63	20.78
Ectal facet width	23.14	27.50	14.80
Head height	22.05	23.40	13.09
Head width	28.64	32.61	18.16
Lateral body height	31.82	30.83	–
Lateral trochlear length	34.75	38.32	–
Medial body height	28.76	33.08	20.50
Medial trochlear length	33.64	40.22	24.70
Neck length	30.28	30.71	20.12
Sustentacular facet length	34.97	36.34	22.24
Sustentacular facet width	15.63	19.27	10.87
Trochlear width	25.42	29.44	–

movements (Argot 2002; Candela and Picasso 2008). In this case, *Neoepiblema* would have had movements of the hindlimb more parasagittal than in extant chinchilloids. In *Phoberomys*, the position of the lesser trochanter, more medial than in *Neoepiblema*, may be advantageous to provide a powerful flexion of the hip joint and vertebral column when the leg is fixed in position. This aspect would provide an advantage to anchor firmly in the sub-

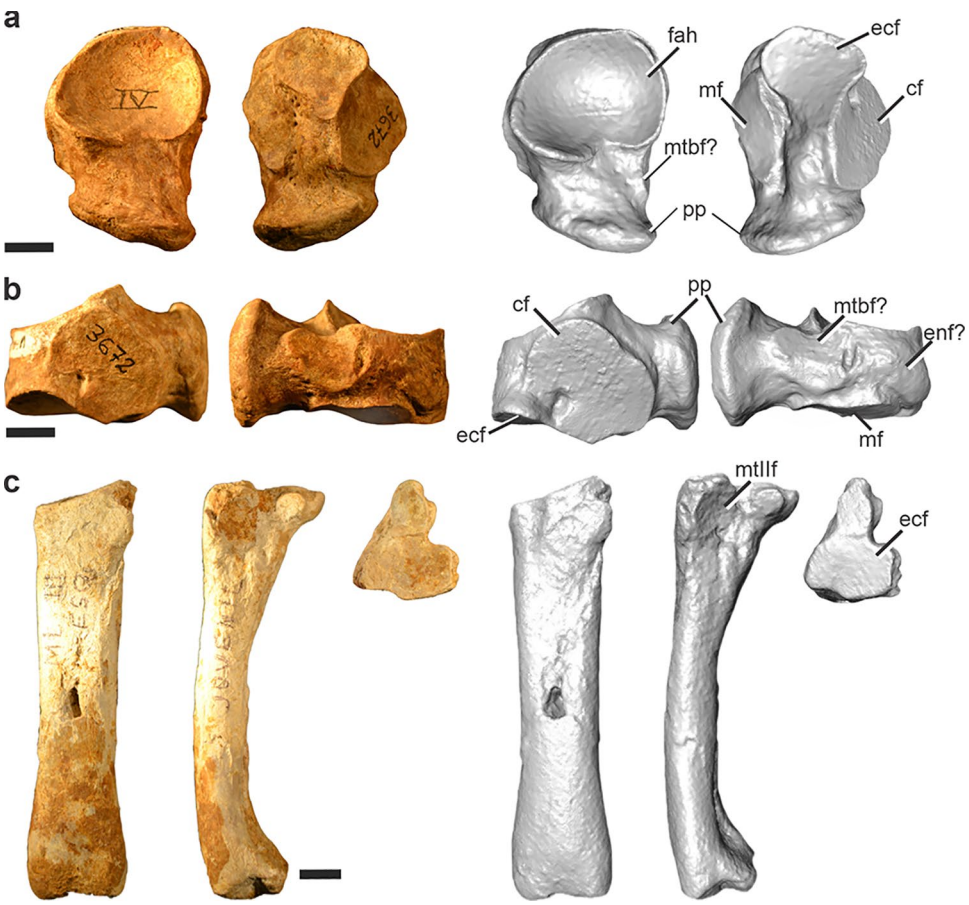

Fig. 13 Photographs (left) and three-dimensional models (right) of the right navicular (UFAC 3672) (**a**. in proximal and distal views; **b**. lateral and medial views) and left metatarsal III (UFAC 2116) (**c**, in dorsal, lateral, and proximal views) of *Neoepiblema acreensis*. *Abbreviations*: *cf*, cuboid facet; *ecf*, ectocuneiform facet; *enf*?, entocuneiform facet?; *fah*, facet for the astragalar head; *mf*, mesocuneiform facet; *mtbf*?, medial tarsal bone facet?; *pp*, plantar process of the navicular; *mtIIf*, metatarsal II facet. Scale bars equal 10 mm

Table 7 Measurements (in mm) of the navicular of *Neoepiblema acreensis*

Measurement	UFAC 3672
Length	47.60
Width	33.45
Plantar process length	20.69
Body length	26.90

strate and resist the forces generated during digging or food manipulation. Thus, it would be useful to resist the large forces during the maintenance of posture in association to the large body size of this giant rodent.

The shaft of the femur of *Neoepiblema* is straight, different from the specimen DGM 601-M (*Phoberomys* sp.), which is slightly curved. This curvature may be related to the predictability of strain patterns, restricting the directional variability of bending loads, which could be related to the larger body size (Bertram and Biewener 1988) of *Phoberomys*.

The distal region of the femur of *Neoepiblema*, as in extant chinchillids and *Phoberomys* (but see above commentaries about *P. pattersoni* and taphonomic influence), shows the transverse diameter equivalent to or slightly larger than the craniocaudal diameter. The morphology of the distal epiphysis of the femur, associated with the depth of the knee joint, expresses the amount and type of forces to which this joint is subjected (Candela and Picasso 2008). A deep distal

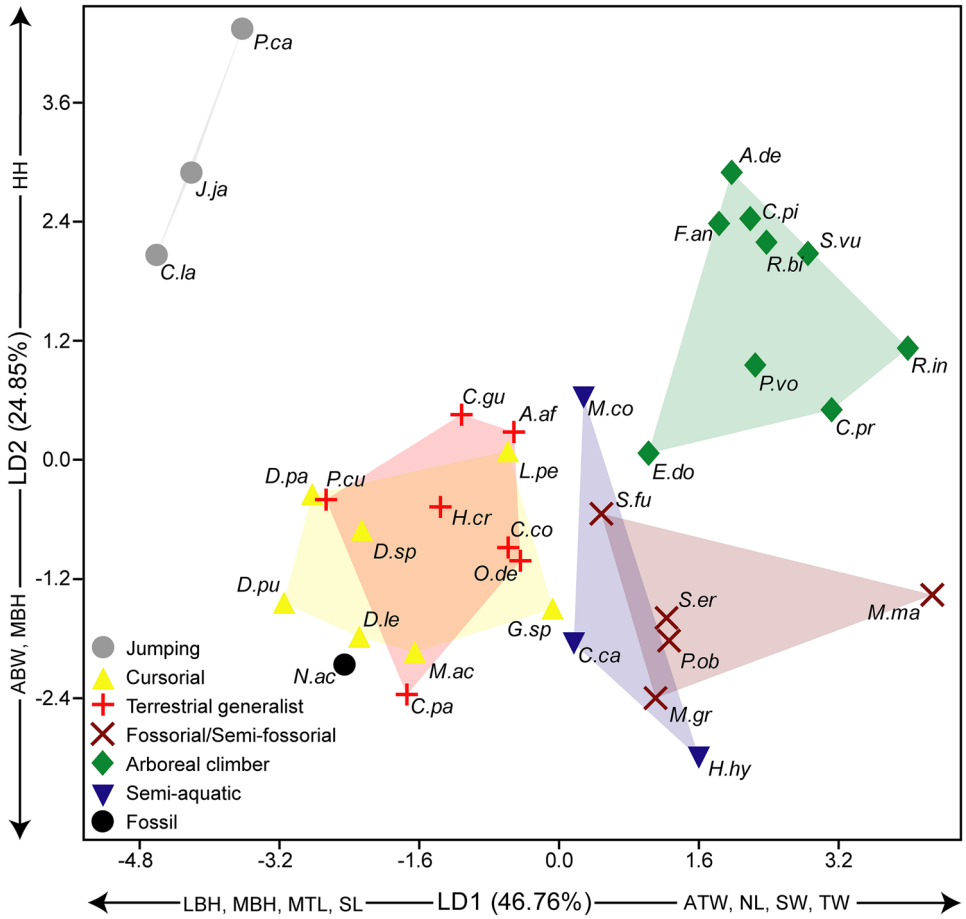

Fig. 14 Linear discriminant analysis (LD1 and LD2) of locomotory groups based on mean log-shape ratios of linear measurements of the astragalus taken from Ginot et al. (2016) and the positioning of *Neoepiblema acreensis* (=*N.ac*) in comparison to the extant species. *Abbreviations: A.de, Anomalurus derbianus; A.af, Atherurus africanus; C.pi, Capromys pilorides; C.ca, Castor canadensis; C.co, Cavia cobaya; C.la, Chinchilla lanigera; C.pr, Coendou prehensilis; C.gu, Ctenodactylus gundi; C.pa, Cuniculus paca; D.le, Dasyprocta leporina; D.pu, Dasyprocta punctata; D.pa, Dolichotis patagonum; D.sp, Dolichotis* sp.*; E.do, Erethizon dorsatum; F.an, Funisciurus anerythrus; G.sp, Gerbillus* sp.*; H.hy, Hydrochoerus hydrochaeris; H.cr, Hystrix cristata; J.ja, Jaculus jaculus; L.pe, Lagidium peruanum; M.ma, Marmota marmota; M.gr, Microtus gregalis; M.co, Myocastor coypus; M.ac, Myoprocta acouchi; O.de, Octodon degus; P.ca, Pedetes capensis; P.cu, Proechimys cuvieri; P.ob, Psammomys obesus; P.vo, Pteromys volans; R.bi, Ratufa bicolor; R.in, Ratufa indica; S.vu, Sciurus vulgaris; S.er, Spalax erhenbergi; S.fu, Spermophilus fulvus*

Table 8 Measurements (in mm) of the metatarsal III of *Neoepiblema acreensis*

Measurement	UFAC 2116
Length	93.86
Transverse diameter at mid-shaft	17.53
Proximal end width	21.35
Proximal end length	27.59

femoral epiphysis (as occurs in cursors) projects the patella (attachment site of the *m. quadriceps femoris* complex) cranially. This pattern increases the lever arm of the *m. quadratus femoris* for the extension of the knee and, consequently, generates more powerful flexion of the hip and extension of the knee, consistent with efficient propulsion during terrestrial locomotion (Candela and Picasso 2008). On the other hand, neoepiblemids, chinchillids, and to a greater degree, extant erethizontids, show a shallower distal femoral epiphysis than in cursorial caviomorphs, which may indicate a more habitually flexed hindlimb (Sargis 2002b; Candela and Picasso 2008). In the case of neoepiblemids, this morphology would generate a greater resistance to the application of great forces generated at the level of the knee joint, subject to support the great weight of these species. It would also provide a strong area to withstand the forces generated during occasional digging, food manipulation, and maintenance of posture in relation to the large size of the animal.

The tibial crest is the insertion area of *m. gracilis* (a limb adductor of the hip joint and flexor of the knee) and *m. semitendinosus* (extensor of the hip joint and flexor of the knee).

Table 9 Correlation (r) of variables with the linear discriminants 1 and 2

Astragalar measurements	LD1	LD2
Astragalus body width (ABW)	-0.095	**-0.349**
Astragalus total length (ATL)	-0.120	0.077
Astragalus total width (ATW)	**0.348**	-0.074
Ectal facet length (EL)	0.323	0.165
Ectal facet width (EW)	-0.059	0.021
Head height (HH)	0.156	**0.555**
Head width (HW)	-0.092	-0.110
Lateral body height (LBH)	**-0.496**	-0.103
Lateral trochlear length (LTL)	-0.224	0.028
Medial body height (MBH)	**-0.548**	**-0.573**
Medial trochlear length (MTL)	**-0.591**	-0.327
Neck length (NL)	**0.377**	0.286
Sustentacular facet length (SL)	**-0.425**	0.122
Sustentacular facet width (SW)	**0.614**	0.183
Trochlear width (TW)	**0.401**	0.128

Significant correlations ($P < 0.05$) are presented in bold

The tibial crest of *Neoepiblema* is distally extended almost to the middle of the shaft, unlike the condition present in some caviomorphs that have a more proximal location of the crest. A distally extended crest increases the mechanical advantage (by increasing the moment arm) of the *m. gracilis* and *m. semitendinosous*, which would produce powerful extension and adduction of the limb and flexion of the knee. Thus, the configuration of the tibial crest indicates a powerful, rather than rapid, hip extension and knee flexion for *Neoepiblema*, traits that would not be suitable for a cursor. Similarly, the tibial features of *P. pattersoni* also show a configuration appropriate for large ambulatory species, not specialized runners.

The distal epiphysis of the tibia indicates that the ankle joint of *Neoepiblema* was possibly relatively restrictive (less mediolaterally mobile than in arboreal forms, for example; Candela and Picasso 2008; Candela et al. 2012), due to the presence of well-marked (concave) tibial facets for the astragalar trochlea separated by a prominent ridge as well as the distal tibial spine that restricts the lateral movements and complete dorsiflexion at the upper ankle joint (Candela and Picasso 2008; García-Esponda and Candela 2010; Candela et al. 2012).

The ridges on the astragalus are slightly asymmetrical and separated by a well-marked groove, which differs from arboreal rodents (in which the ridges are more asymmetrical, comparatively less developed, and with a shallow groove), and also from cursorial taxa, which have symmetrical ridges (Candela and Picasso 2008; Ginot et al. 2016; Candela et al. 2017). The astragalar neck is craniomedially oriented, not cranially as *Dolichotis patagonum* and *H. hydrochaeris*, but less medially oriented than in erethizontids (Candela and Picasso 2008; Ginot et al. 2016). The astragalar head is transversally elongated, similar to the pattern of *H. hydrochaeris*, differing from erethizontids, which show a globular head (Candela and Picasso 2008), and from *L. maximus*, *C. lanigera*, and *D. branickii*, in which it is transversely narrower. Rodents with the astragalar head oriented parallel to the parasagittal plane (e.g., caviids) have movements restricted to flexion–extension, while taxa with a medial orientation of the head are able to produce lateral movements (e.g., erethizontids). Concerning this trait, *Neoepiblema* could have some degree of lateral movement of the foot, more accentuated in *N. horridula*, which shows a shorter astragalar head than *N. acreensis*, but not as in erethizontids. The craniocaudally oriented sustentacular facet of *Neoepiblema* also improves the parasagittal movements (Candela and Picasso 2008). The combination of features present in the astragalar morphology of *Neoepiblema* is consistent with the pattern observed in terrestrial generalists (see previous discussion). However, the ecomorphological analysis (Fig. 14) points to a more cursorial habit. Still, the extensive morphological overlap between generalist and cursorial

Table 10 Body mass estimates based on the diameter of the long bones of *Neoepiblema*. Equations from Biknevicius et al. (1993)

Taxon/anatomical element	Specimen	Measurement (mm)	Equation	Body mass (kg)
N. acreensis				
Humerus	UFAC 3549	32.73	–1.467 + 2.484 (logX)	197.75
Humerus	UFAC 5076	29.09	–1.467 + 2.484 (logX)	147.55
Femur	UFAC 2574	33.36	–1.678 + 2.518 (logX)	143.71
Femur	UFAC 4907	34.60	–1.678 + 2.518 (logX)	157.54
Femur	UFAC 2937	33.77	–1.678 + 2.518 (logX)	148.20
N. horridula				
Femur	UFAC 2737	24.11	–1.678 + 2.518 (logX)	63.44

caviomorphs in this approach (Ginot et al. 2016) makes it difficult to distinguish between these two habits with confidence solely based on it.

For the navicular, we calculated the index 1 of Candela et al. (2017). As such, the ratio of the plantar process of the navicular length (20.69 mm) to the navicular body length (26.9 mm) results in a value of 0.76. This value is low, suggesting a short plantar process of the navicular, as found in extant octodontoids, erethizontids, and chinchillids by Candela et al. (2017), in contrast to cavioids, which are cursorial forms that have a larger process and higher index values. In cavioids, the plantar process would act as a buttress, while in the chinchilloids, such as in *C. lanigera* (jumper) and *L. maximus* (digger, which requires a strengthened plantar region to withstand impacts), the plantar process is not as well developed, and the strengthening of the plantar region is given by the presence of a highly developed Mt II tuber and a sesamoid, also highly developed. Hence, among caviomorphs, at least two different "strategies" to strengthen the plantar region seem to have evolved (Candela et al. 2017). More fossils of the foot of *Neoepiblema* are necessary to analyze if this rodent shows a "strategy" to strengthen the plantar region of the foot similar to that of extant chinchilloids.

Unlike *C. lanigera* and *L. maximus*, the relatively short metatarsals of *Neoepiblema* (judging by the Mt III) and *Phoberomys* (Horovitz et al. 2006: fig. 14) would provide a more effective resultant force for locomotion at the expense of velocity, which would result in short and powerful strides (Candela et al. 2017). Short metatarsals in these neoepiblemids indicate that they are not highly specialized for running or leaping habits.

Candela et al. (2017) analyzed the tarsal-metatarsal morphology of caviomorph rodents and recognized two main tarsal-metatarsal patterns (TMPs). TMPI presents traits that facilitate movements of the foot at different levels. In TPMII, the morphological features stabilize joints and restrict movements to the parasagittal plane. Several features of the tarsal-metatarsal pattern of *Neopiblema* are similar to TMPI. The astragalar body is relatively wide, the astragalar head is somewhat medially oriented with respect to the astragalar trochlea, the astragalar neck is relatively short, and the astragalomediotarsal facet of the astragalar head for the medial tarsal bone is well developed, which suggests that the medial tarsal was relatively well developed. Additionally, the plantar process of the navicular is poorly developed. Based on the relative size of the navicular facets, the cuboid was larger than the ectocuneiform. Finally, the metatarsals are relatively short. According to Candela et al. (2017), among chinchilloids, *Lagostomus* shows a typical TMPII, but *Lagidium* and *Chinchilla* partially depart from this pattern. *Neoepiblema* shows a pattern more similar to the typical TMPI (Candela et al. 2017), being even more generalized than in *Lagidium* and *Chinchilla*.

Functional Traits, Locomotion, and Behavior The forelimb of *Neoepiblema* shows the presence of a well-developed, slightly laterally deflected and distally extended deltopectoral crest, moderate lateral epicondylar ridge, distal articular surface with cylindrical capitulum and faint capitular tail and 'second trochlea', and well developed, proximally oriented olecranon, among other traits. This

Table 11 Parameters and results of the volume-inferred body mass estimates of *Neoepiblema acreensis* based on a digital sculpture with a volume of 0.073 (m^3). *Sources*: [1]Buchner et al. (1997); [2]Garret (1968); [3]Kodama (1971)

Taxon	Density (kg/m3)	Density source	Body mass (kg)
Equus caballus[1]	893	Weighted mean of segment densities (n = 1)	65.32
Bos primigenius[2]	1056	Mean density of right half of beef steer carcass (n = 48)	77.24
Ovis aries[2]	912	Mean carcass density (including fat) (7 studies)	66.71
Sus scrofa[2]	943	Mean carcass density (including fat) (6 studies)	68.98
Mesocricetus auratus[3]	1049	Mean carcass density of male hamsters (n = 34)	76.73

combination of traits suggests that *Neoepiblema* would have a forelimb with the capacity of a powerful flexion. The forelimb was not fully extended and had powerful pectoral and triceps musculature, with substantial movements of the radial head. Thus, it may have had the ability to produce movements of pronation/supination and perhaps a hand that was able to grasp. The moderately deep olecranon fossa and the absence of a supratrochlear foramen suggest that it could not fully extend the elbow as in cursorial forms. However, the depth of the olecranon fossa suggests that they would have a considerable capacity for extension, this not being a limiting factor in digging or swimming. A relatively well-developed olecranon is also compatible with digging abilities. The orientation of the olecranon suggests a crouched position of the forelimb. Therefore, the *Neoepiblema* forearm exhibits a set of characters that are compatible with food manipulation but also swimming and/or digging.

Regarding the pelvic girdle and hindlimb, the innominate shows a well-developed rectus femoris tuberosity, and the hindlimb is characterized by a femur with a well-developed greater trochanter extending further proximally than the femoral head and protruding laterally, lesser trochanter caudomedially oriented, and distal epiphysis with a transverse diameter equivalent to or slightly larger than the craniocaudal diameter. The tibia has a distally extended tibial crest and its distal articular face shows marked trochlear facets; and the astragalus has asymmetrical ridges, craniomedially oriented neck and astragalar head, and a transversally extended head. This combination of traits indicates a predominance of parasagittal movements, a thigh with powerful propulsive musculature, and some degree of lateral movements of the foot, features that are expected in ambulatory species. These traits are also compatible with ability to dig and swim, which tend to be related to strong joints and powerful hindlimb musculature. Lateromedial extension of the elbow and knee could have been advantageous to support the great efforts generated on these joints associated with the great weight of these rodents, reaching its maximum expression in *Phoberomys*.

Based on the sedimentary context in which neoepiblemids have been found, it has been inferred that they probably inhabited water-related environments, like swamps, lakes, or rivers, being possibly semiaquatic or using these places to forage (Sánchez-Villagra et al. 2003). Their Middle to Late Miocene fossil record is restricted to few localities where sedimentary deposition occurred in wet conditions and paleoenvironments that include lakes, rivers, and swamps. The oldest record of *Neoepiblema* comes from the Middle Miocene of the local fauna of the Fitzcarrald Arch, Peru (Tejada-Lara et al. 2015), where the paleoenvironment was related to the mega-wetland Pebas, whose main components were tropical forest and swamps (Hoorn et al. 2010). Late Miocene records are restricted to the Mesopotamian region of Argentina (Ituzaingó Formation), Venezuela (Urumaco Formation), and Brazil (Solimões Formation). The fossils from the Ituzaingó Formation were preserved in fluvial environments representative of hot and wet climates (Cione et al. 2000). In the Urumaco Formation, the evidence indicates wet coastal environments that consisted of shallow water lagoons isolated from the coast by sandy barriers (Horovitz et al. 2010). In Solimões Formation deposits, the upper levels were deposited in wetlands associated with systems of megafans, lakes, and swamps. An abundant concentration of fossils of *N. acreensis* was recovered from the Niterói locality, Acre River. Palynology of this site indicates the presence of swamp environments during the deposition of these layers (Latrubesse et al. 2010). The youngest record of a neoepiblemid comes from the Pliocene of San Gregorio, Falcón State, Venezuela, which also documents the presence of permanent freshwater systems (Vucetich et al. 2010; Carrillo-Briceño et al. 2021). Thus, the available sedimentary and paleoclimatic information indicates that the distribution of neoepiblemids during the Neogene was restricted to environments with hot and wet conditions, suggesting a relationship between these rodents and permanent aquatic environments. Vucetich et al. (2010) and Nasif et al. (2013) noticed that in other Argentinean Upper Miocene strata deposited under dry conditions there is an abundant record of rodent fossils, but neoepiblemids are absent.

The traits observed in the postcranial bones analyzed here permit us to infer that rodents of the genus *Neoepiblema* were possibly ambulatory, being mainly terrestrial but with the faculty to dig or swim (Fig. 15). The postcranial features observed here are consistent with the capacity to swim, although it is not possible to confidently infer this habit. Semiaquatic rodents show traits such as a reduced hindlimb elements (compared to terrestrial relatives), with bones showing negative allometry with the body size, long feet, and long tail (Stein 1988; Samuels and Van Valkenburgh 2008; but see García-Esponda and Candela 2016). However, in the capybara, the opposite is observed. This rodent shows short metatarsals and low pes length index (Mt III length/femur length), features associated with its quadrupedal paddling swimming (García-Esponda and Candela 2016). Unfortunately, the fragmentary material does not permit proper assessment of limb bone indexes for *Neoepiblema* (Elissamburu and Vizcaíno 2004; Samuels and Van Valkenburgh 2008). Additionally, it is not possible to confidently associate the bones to a single individual. Some indexes require comparisons of dimensions between two bones, and using data from different individuals can result in inaccurate results.

Notwithstanding, Samuels and Valkenburgh (2008) argued that rodents have an impressive array of locomotor

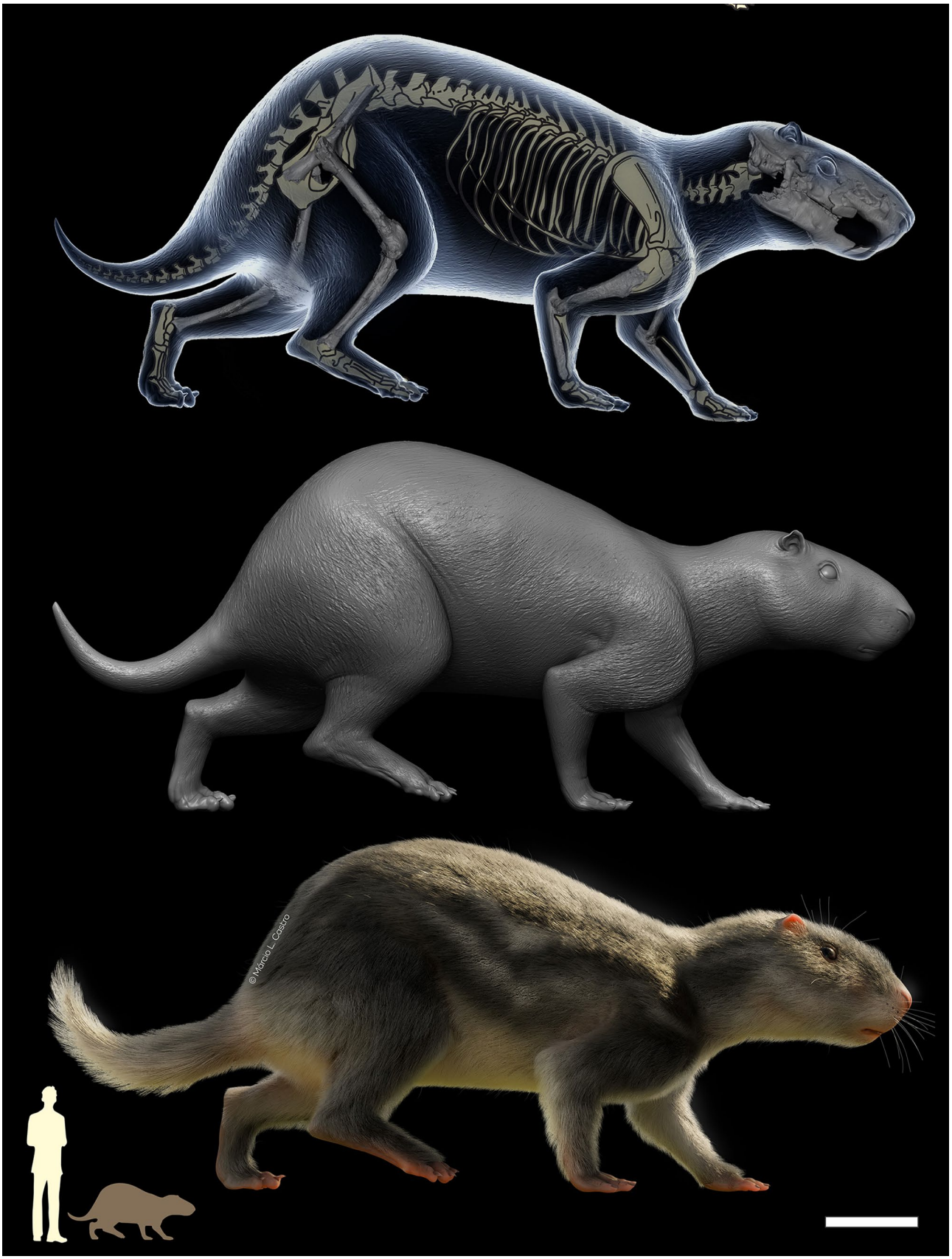

Fig. 15 Tridimensional sculpture and life reconstruction of *Neoepiblema acreensis*. 3D reconstruction by Márcio L. Castro. Scale bar equal 15 cm

behaviors without extensive morphological specializations. Hence, although the osteological characteristics indicate that *Neoepiblema* would have the faculty for such locomotor behaviors, it does not mean that these rodents presented them in life (see Vizcaíno et al. 2016).

Body Mass Estimates of *Neoepiblema*

The mass estimates based on the diameter of the humerus and femur of *Neoepiblema acreensis* revealed a body mass of more than 150 kg on average. However, these results are much higher than those estimated by Ferreira et al. (2020) based on the average of craniodental measurements of *N. acreensis* (79.75 kg). The results of Ferreira et al. (2020) also fall closer to the body mass range estimated by the volumetric approach (65.3 – 77.2 kg). Both the volume-inferred body mass and the estimate based on craniodental measurements (Ferreira et al. 2020) seem to be more reasonable than estimates based on the long bone diameters for the taxon. Indeed, the skull of *N. acreensis* is not substantially larger than that of an extant capybara, whose body mass averages around 40–60 kg in adults (Mones and Ojasti 1986). This discrepancy in body mass estimates based on long bone diameter *versus* other methods was discussed by Hopkins (2008) and Millien and Bovy (2010), and the case-specific 'single-bone problem' of bivariate regressions is recognized in body mass estimates of other animal groups (Brassey and Sellers 2014; Hopkins 2018; Campione & Evans 2020), not being a problem exclusive of rodents.

There is an ongoing discussion in the literature concerning the different methodologies adopted to estimate body masses of extinct taxa (see Campione and Evans 2020 for a comprehensive review; Croft et al. 2020). Though digital sculptures may suffer from biases related to the paleoartistic view of an extinct animal, bivariate regressions, or extant-scaling (Campione and Evans 2020) suffer from the so-called 'single bone problem' (Brassey and Sellers 2014), for the reliance on a single bone measurement as predictive of body mass can sometimes result in considerable under- or overestimation, due to sampling, allometry, or other issues. Whatever the reason, both methodologies have their uses and biases, and, at least for *Neoepiblema*, the estimate based on craniodental measurements using allometric equations and the volume-inferred body mass generated similar results, adding confidence to both methodologies in this case.

Fossil Record and Paleoecological Remarks

Most of the fossils analyzed here come from concentrations found in two localities: Niterói and Talismã, both preserving elements of several individuals (Kerber et al. 2017a, b). Kerber et al. (2017b) suggested that some of those fossils display marks of digestion, which could evidence ecological relationships between neoepiblemids (and other rodents) and Miocene Amazonian predators, such as the giant crocodilians. Here, additional evidence is presented based on at least one femur (Fig. 16) from Talismã locality that shows marks quite similar to the pattern reported in bones and fossils of small mammals that have been digested (e.g., Fernández-Jalvo and Andrews 1992; Denys et al. 1995; Montalvo and Tallade 2009; Montalvo et al. 2012).

The concentration of fossils of several individuals in the same place favors the hypothesis that *Neoepiblema* was gregarious or congregated, as in extant closely related chinchilloids *Lagostomus maximus* (Jackson et al. 1996), *Chinchilla* (Roach and Kennerley 2016a, b), and *Dinomys branickii* (Roach 2017). However, such inferences must be further addressed, mainly with controlled excavations.

Summary, Conclusions, and Future Perspectives

We studied the morphology of late Miocene postcranial bones of *Neoepiblema,* searching for paleobiological information. Our main observations are summarized as follows:

Fig. 16 Right femur in caudal view of *Neoepiblema horridula* (UFAC 2739) from the Talismã locality, Purus River, showing possible marks of digestion (indicated by arrows). Scale bar equals to 10 mm

i) In comparison with other chinchilloids, the forelimb morphology of *Neoepiblema* shares similarities with *Phoberomys*, such as the presence of a deltopectoral crest extended from the proximal region to the midportion of the diaphysis (or distally passing this region in *P. pattersoni*), not tapering cranially, and absence of supratrochlear foramen. Such traits are different from the extant chinchilloids *Lagostomus maximus, Chinchilla lanigera,* and *Dinomys branickii*, and from the Early Miocene *Perimys*. However, the ulna of *Phoberomys pattersoni* shows the olecranon slightly cranially oriented in relation to the main axis of the shaft, distinct from *Neoepiblema* and *Perimys*, in which the olecranon is oriented in line with the main axis. The femoral anatomy of *Neoepiblema* and *Phoberomys* shares with *L. maximus* and *C. lanigera* a greater trochanter extending further proximally than the femoral head and protruding laterally. This pattern is distinct from *D. branickii*, in which the greater trochanter does not extend as far proximally beyond the femoral head, and there is no lateral projection. In *Neoepiblema*, the lesser trochanter is caudomedially oriented, but less medially than in *Phoberomys*. In the chinchillids *L. maximus* and *C. lanigera,* this structure is medially protruding and can be observed in cranial view. *Neoepiblema* and *Phoberomys* also share a tibia with a distally extended tibial crest and the astragalus with the body transversally longer than proximodistally. No significant differences are observed in the postcranial bones of *N. acreensis* and *N. horridula*, except that the bones of the latter taxon are smaller and more gracile. In sum, the comparative study of *Neoepiblema* and *Phoberomys* reveals several similarities and differences in the postcranial characters of extinct and extant chinchilloids. These characters emerge as a valuable source of information for future phylogenetic analyses.

ii) The analyzed features are consistent with the limb morphology of an ambulatory rodent with faculty to dig or swim. The sedimentary evidence suggests that these rodents lived in water-related environments. Although it is here inferred that *Neoepiblema* may have been able to swim, the data do not allow a firm statement that they were semiaquatic. *Phoberomys* could be an ambulatory rodent similar to *Neoepiblema* and may have had swimming abilities. Several characteristics of *Phoberomys* are associated with its large size. Among these are the wide joints for supporting the loads generated by the weight of the animal during the walk. Notably, several of the traits of this genus converge with those found in species with climbing abilities (e.g., the convexity of the caudal border of the proximal region of the ulna, lesser trochanter oriented more medially, medially displaced astragalar head, lateromedially expanded elbow, and knee joints, and distally expanded deltoid crest and tibial crest).

iii) Body mass estimates of *N. acreensis* based on allometric equations of the humerus (~172.65 kg) and femur (~149.81 kg) result in values much higher than the estimates based on craniodental measurements (~79.75 kg) and the volume-inferred body mass (65.3–77.2 kg). The two latter approaches seem to provide more reasonable results when compared to estimates based on the postcranial bone diameters.

iv) Finally, it is important to point out that the postcranial elements were found in the same levels as craniodental remains. However, there is no taphonomic information on the collection of these bones. Hence, the further discovery of a skeleton of a single individual will help to better understand the postcranium of *Neoepiblema* and further clarify any potential biases produced by the analysis of isolated bones.

Supplementary Information The online version contains supplementary material available at https://doi.org/10.1007/s10914-021-09567-4.

Acknowledgments The authors thank the UFAC team (A Maciente, A Ranzi, E Guilherme, J Bocquentin-Villanueva, JCR dos Santos, JP Souza-Filho) that collected the studied material housed in UFAC; MR Sánchez-Villagra, who shared with us information about *Phoberomys pattersoni*; S Ginot, for his help with LDA analysis; RD Rocha Machado (DMG), A. Kramarz and S. Alvarez (MACN) for access to the collections under their care; Editor DA Croft and two anonymous referees for their useful comments that greatly improved the manuscript.

Funding LK is supported by the Conselho Nacional de Desenvolvimento Científico e Tecnológico (CNPq 422568/2018–0; 309414/2019–9). JDF is supported by the Coordenação de Aperfeiçoamento de Pessoal de Nível Superior–Brasil (CAPES)–Finance Code 001. JB has a postdoctoral fellowship at the Universidade Estadual do Norte Fluminense (UENF).

Declarations

Competing Interests The authors have no conflicts of interests related to this research.

References

Alexander RMN (1985) Mechanics of posture and gait of some large dinosaurs: Zool J Linnean Soc 83, p. 1–25. https://doi.org/10.1111/j.1096-3642.1985.tb00871.x

Ameghino F (1886) Contribuciones al conocimiento de los mamíferos fósiles de los terrenos terciarios antiguos del Paraná. Boletín de la Academia de Ciencias de Córdoba 9:1–228.

Ameghino F (1887) Enumeración sistemática de las especies de mamíferos fósiles coleccionados por Carlos Ameghino en los terrenos eocenos de la Patagonia austral y depositados en el Museo de La Plata. Boletín del Museo de La Plata 1:1–26.

Araújo FAP, Sesoko NF, Rahal SC, Teixeira CR, Müller TR, Machado MRF (2013) Bone Morphology of the hind limbs in two caviomorph rodents. Anat Histol Embryol 44:114–123. https://doi.org/10.1111/j.1439-0264.2012.01172.x

Argot C (2001) Functional-adaptive anatomy of the forelimb in the Didelphidae, and the paleobiology of the Paleocene marsupials *Mayulestes ferox* and *Pucadelphys andinus*. J Morphol 247:51–79. https://doi.org/10.1002/1097-4687(200101)247:1<51::AID-JMOR1003>3.0.CO;2-#.

Argot C (2002) Functional-adaptive analysis of the hindlimb anatomy of extant marsupials and paleobiology of the Paleocene marsupials *Mayulestes ferox* and *Pucadelphys andinus*. J Morphol 253:76–108. https://doi.org/10.1002/jmor.1114.

Bates KT, Falkingham PL, Macaulay S, Brassey C, Maidment SCR (2015) Downsizing a giant: re-evaluating *Dreadnoughtus* body mass. Biol Lett 11:20150215. https://doi.org/10.1098/rsbl.2015.0215

Bertram JEA, Biewener AA (1988) Bone curvature: Sacrificing strength for load predictability? J Theor Biol 131:75–92. https://doi.org/10.1016/s0022-5193(88)80122-x.

Biknevicius AR (1993) Biomechanical scaling of limb bones and differential limb use in caviomorph rodents. J Mammal 74:95–107. https://doi.org/10.2307/1381908

Biknevicius AR, McFarlane DA, MacPhee RD (1993) Body size in *Amblyrhiza inundata* (Rodentia: Caviomorpha), an extinct megafaunal rodent from the Anguilla Bank. West Indies: Estimates and implications. Am Mus Novit 3079:1–25.

Bissaro-Júnior MC, Kerber L, Crowley J, Ribeiro AM, Ghilardi RP, Guilherme E, Negri FR, Hsiou AS. 2019. Detrital zircon U-Pb geochronology constrains the age of Brazilian Neogene deposits from western Amazonia. Palaeogeograp Palaeoclimatol Palaeoecol 516:64–70. https://doi.org/10.1016/j.palaeo.2018.11.032

Bocquentin-Villanueva JB, Souza-Filho JP, Negri FR (1990) *Neoepiblema acreensis*, sp. n. (Mammalia, Rodentia) do Neógeno do Acre, Brasil. Bol Mus Para Emílio Goeldi Ciênc 2:65–72.

Bondesio P, Pascual R, Vucetich MG (1975) Los Neoepiblemidae (Rodentia, Caviomorpha): su caracterización y sus relaciones filogenéticas con los Chinchillidae. Actas del Primer Congreso Argentino de Paleontología y Bioestratigrafía, Tomo 2: 431–447.

Brassey CA (2017) Body-mass estimation in paleontology: a review of volumetric techniques. The Paleontological Society Papers 22: 133–156. https://doi.org/10.1017/scs.2017.12

Brassey CA, Sellers WI (2014) Scaling of convex hull volume to body mass in modern primates, non-primate mammals and birds. PLoS ONE 9:e91691. https://doi.org/10.1371/journal.pone.0091691

Buchner HHF, Savelberg HHCM, Schamhardtt HC, Barneveld A (1997) Inertial properties of Dutch Warmblood horses. J Biomech 30: 653–658. https://doi.org/10.1016/S0021-9290(97)00005-5

Busker F, Dozo MT, Soto IM (2020) New remains of *Cephalomys arcidens* (Rodentia, Caviomorpha) and a redefinition of the enigmatic Cephalomyidae. J Syst Palaeontol 18:1589–1629. https://doi.org/10.1080/14772019.2020.1796833

Campione NE, Evans DC. 2020. The accuracy and precision of body mass estimation in non-avian dinosaurs. Biol Rev 95:1759–1797. https://doi.org/10.1111/brv.12638

Candela A Picasso MBJ (2008) Functional anatomy of the limbs of Erethizontidae (Rodentia, Caviomorpha): Indicators of locomotor behavior in Miocene porcupines. J Morphol 269:552–593. https://doi.org/10.1002/jmor.10606.

Candela AM, Muñoz NA, García-Esponda CM (2017) The tarsalmetatarsal complex of caviomorph rodents: Anatomy and functional adaptive analysis. J Morphol 278:828–847. https://doi.org/10.1002/jmor.20678

Candela AM, Muñoz NA, García-Esponda CM (2018) Paleobiology of the basal hydrochoerine *Cardiomys* Ameghino, 1885 (Rodentia, Caviomorpha, late Miocene, South America) as inferred from its postcranial anatomy. J Paleontol 92:911–919. https://doi.org/10.1017/jpa.2018.12

Candela AM, Rasia LL, Perez ME (2012) Paleobiology of Santacrucian caviomorph rodents: a morphofunctional approach. In: Vizcaíno SF, Kay RF, Bargo MS (eds) Early Miocene Paleobiology in Patagonia: High-Latitude Paleocommunities of the Santa Cruz Formation. Cambridge University Press, Cambridge, pp 287–305.

Carrillo JD, Sánchez-Villagra M (2015) Giant rodents from the Neotropics: diversity and dental variation of late Miocene neoepiblemid remains from Urumaco, Venezuela. Palaontol Z 89(4):1057–1071. https://doi.org/10.1007/s12542-015-0267-3

Carrillo-Briceño JD, Sánchez R, Scheyer TM, Carrillo JD, Delfino M, Georgalis GL, Kerber L, Ruiz-Ramoni D, Birindelli LO, Cadena EA, Rincón AF, Chavez-Hoffmaizer M, Carlini AA, Carvalho MR, Jaramillo C, Sánchez-Villagra MR (2021) A Pliocene-Pleistocene continental vertebrate fauna from northern South America (Venezuela). Swiss J Palaeontol 140(9):1–76. https://doi.org/10.1186/s13358-020-00216-6

Cignoni P, Callieri M, Corsini M, Dellepiane M, Ganovelli F, Ranzunglia G (2008) MeshLab: an open-source mesh processing tool. In: Scarano R, De Chiara R, Erra U (eds) Proceedings of the EG It 2008 - Eurographics Italian Chapter Conference. The Eurographics Association, Salerno, pp 129–136.

Cione AL, Azpelicueta MM, Bond M, Carlini AA, Casciotta J, Cozzuol M, de la Fuente M, Gasparini Z, Goin F, Noriega J, Scillato-Yané G, Soibelzon L, Tonni EP, Verzi D, Vucetich MG (2000) Miocene vertebrates from Entre Ríos, eastern Argentina. In: Azeñolaza F, Herbst R (eds) El Neógeno de Argentina. INSUGEO – Serie de Correlación Geológica 14, Tucumán, pp 191–237.

Claude J (2008) Morphometrics with R. Berlin, Springer Science and Business Media.

Cozzuol M (2006) The Acre vertebrate fauna: diversity, geography and time. J S Am Earth Sci 21:185–203. https://doi.org/10.1016/j.jsames.2006.03.005

Croft DC, Gelfo JN, López GM (2020) Splendid innovation: the extinct South American native ungulates. Annu Rev Earth Planet Sci 48:11.1–11.32. https://doi.org/10.1146/annurev-earth-072619-060126

Denys C, Fernandez-Jalvo Y, Dauphin Y (1995) Experimental Taphonomy: preliminary results of the digestion of micromammal bones in the laboratory. C R Acad Sci 321:803–809.

Elissamburu A, Vizcaíno SF (2004) Limb proportions and adaptation in caviomorph rodents. J Zool 262:145–159. https://doi.org/10.1017/S0952836903004485

Fernández-Jalvo Y, Andrews P (1992) Small Mammal Taphonomy of Gran Dolina, Atapuerca (Burgos), Spain. J Archaeol Sci 19:407–428.

Ferreira JD, Negri FR, Sánchez-Villagra MR, Kerber L (2020) Small within the largest: brain size and anatomy of the extinct *Neoepiblema acreensis*, a giant rodent from the Neotropics. Bio Lett 16: 20190914. https://doi.org/10.1098/rsbl.2019.0914

Fujiwara S (2009) Olecranon orientation as an indicator of elbow joint angle in the stance phase, and estimation of forelimb posture in extinct quadruped animals. J Morphol 270:1107–1121. https://doi.org/10.1002/jmor.10748

García-Esponda CM, Candela AM (2010) Anatomy of the hindlimb musculature of the cursorial caviomorph *Dasyprocta azarae* Lichtenstein, 1823 (Rodentia, Dasyproctidae): functional and evolutionary significance. Mammalia 74:407–422. https://doi.org/10.1515/mamm.2010.042

García-Esponda CM, Candela AM (2016) Hindlimb musculature of the largest living rodent *Hydrochoerus hydrochaeris* (Caviomorpha): Adaptations to semiaquatic and terrestrial styles of life. J Morphol 277:286–305. https://doi.org/10.1002/jmor.20495

García-Esponda CM, Calanoce AR, Candela AM (2021) Brachiocephalic muscular arrangements in cavioid rodents (Caviomorpha): a

functional, anatomical, and evolutionary study. J Mamm Evol 28:529–541. https://doi.org/10.1007/s10914-020-09529-2

Garrett WN (1968) Experiences in the use of body density as an estimator of body composition in animals. In: Nacional Researh Council (ed) Body Composition In Animals and Man. Proceedings of a Symposium Held May 4, 5, and 6, 1967, at the University of Missouri, University of Missouri, Columbia, pp. 170–185. https://doi.org/10.17226/20255

Geiger M, Wilson LAB, Costeur L, Sánchez R, Sánchez-Villagra MR (2013) Diversity and body size in giant caviomorphs (Rodentia) from the northern neotropics – a study of femoral variation. J Vertebr Paleontol 33(6):1449–1456. https://doi.org/10.1080/02724634.2013.780952

Ginot S, Hautier L, Marivaux L, Vianey-Liaud M (2016) Ecomorphological analysis of the astragalo-calcaneal complex in rodents and inferences of locomotor behaviours in extinct rodent species. PeerJ 4:e2393. https://doi.org/10.7717/peerj.2393

Gregory WK (1905) The Weight of the *Brontosaurus*: Science 22 572-572 https://doi.org/10.1126/science.22.566.572

Hildebrand M (1974) Analysis of Vertebrate Structure. New York, John Wiley.

Horovitz I, Sanchez-Villagra MR, Martin T, Aguilera OA (2006) The fossil record of *Phoberomys pattersoni* Mones 1980 (Mammalia, Rodentia) from Urumaco (Late Miocene, Venezuela), with an analysis of its phylogenetic relationships. J Vertebr Paleontol 4(3):293–306. https://doi.org/10.1017/S1477201906001908

Hopkins SSB (2008) Reassessing the mass of exceptionally large rodents using toothrow length and area as proxies for body mass. J Mammal 89:232–243. https://doi.org/10.1644/06-MAMM-A-306.1

Hopkins SSB (2018) Estimation of body size in fossil mammals. In: Croft DA, SU DF, Simpson SW (eds) Methods in Paleoecology: Reconstruction Cenozoic Terrestrial Environments and Ecological Communities. Springer: Vertebrate Paleobiology and Paleoanthropology Series, Switzerland, pp.7–22. https://doi.org/10.1007/978-3-319-94265-0_2

Horovitz I, Sanchez-Villagra MR, Vucetich MG, Aguilera AO (2010) Fossil rodents from the late Miocene Urumaco and Middle Miocene Cumaca formations, Venezuela. In: Sanchez-Villagra MR, Aguilera OA, Carlini AA (eds) Urumaco and Venezuelan Paleontology. Indiana University Press, Bloomington, Indiana, pp 214–232.

Hoorn C, Wesselingh FP, Hovikoski J, Guerrero J (2010) The development of the Amazonian megawetland (Miocene; Brazil, Colombia, Peru, Bolivia). In: Hoorn C, Wesselingh FP (eds) Amazonia: Landscapes and Species Evolution: A look into the past. Wiley-Blackwell, Oxford, pp 123–142.

Jackson JE, Branch LC, Vilarreal D (1996) *Lagostomus maximus*. Mammal Species 543:1-6.

Kerber L, Sánchez-Villagra M (2019) Morphology of the middle ear ossicles in the rodent *Perimys* (Neoepiblemidae) and a comprehensive anatomical and morphometric study of the phylogenetic transformations of these structures in caviomorphs. J Mamm Evol 26:407–422. https://doi.org/10.1007/s10914-017-9422-9

Kerber L, Ferreira JD, Negri FR (2019a) A reassessment of the cranial morphology of *Neoepiblema acreensis* (Rodentia: Chinchilloidea), a Miocene rodent from South America. J Morphol 289:1821-1838. https://doi.org/10.1002/jmor.21067

Kerber L, Negri FR, Sanfelice D (2019b) Morphology of cheek teeth and dental replacement in the extinct rodent *Neoepiblema* Ameghino, 1889 (Caviomorpha, Chinchilloidea, Neoepiblemidae). J Vertebr Paleontol 38(6)e1549061-2. https://doi.org/10.1080/02724634.2018.1549061

Kerber L, Negri FR, Ribeiro AM, Nasif NL, Souza-Filho JP, Ferigolo J (2017a) Tropical fossil caviomorph rodents from the southwestern Brazilian Amazonia in the South American rodent fauna context: systematics, biochronology and paleobiogeography. J Mamm Evol 24:57-70. https://doi.org/10.1007/s10914-016-9340-2

Kerber L, Negri FR, Ferigolo J, Mayer EL, Ribeiro AM (2017b) Modifications of fossils of neoepiblemids and other South American rodents. Lethaia 50(1):149–161. https://doi.org/10.1111/let.12183

Kerber L, Candela AM, Ferreira JD, Pretto FA, Bubadué J, Negri FR (2021) 3D models related to the publication: Postcranial morphology of the extinct rodent *Neoepiblema* (Rodentia: Chinchilloidea): insights on the paleobiology of neoepiblemids. MorphoMuseum. https://doi.org/10.18563/journal.m3.140

Kodama AM (1971) In vivo and in vitro and body water determinations of body fat in the hamster. J Appl Physiol 31: 218–222. https://doi.org/10.1152/jappl.1971.31.2.218

Kraglievich L (1926) Los grandes roedores terciarios de la Argentina y sus relaciones con ciertos géneros Pleistocenos de las Antillas. Anales del Museo Nacional de Historia Natural de Buenos Aires 34:122–135.

Kraglievich L (1932) Diagnosis de nuevos géneros y especies de roedores cávidos y eumegámidos fósiles de la Argentina. Anales de la Sociedad Científica Argentina 114:32–49.

Kraglievich L (1940) Los roedores de la familia extinguida Neoepiblemidae. In: Torcelli AJ, Marelli CA (eds) Obras en Geología y Paleontología. Talleres de Impresiones Oficiales, La Plata, pp. 741–764

Kramarz AG, Bond M, Arnal M (2015) Systematic description of three new mammals (Notoungulata and Rodentia) from the early Miocene Cerro Bandera Formation, Northern Patagonia, Argentina. Ameghiniana 52(6):585–597. https://doi.org/10.5710/AMGH.27.06.2015.2906

Latrubesse EM, Cozzuol M, Silva-Caminha SAF, Rigsby CA, Absy ML, Jaramillo C (2010) The Late Miocene paleogeography of the Amazon Basin and the evolution of the Amazon River system. Earth Sci Rev 99:99–124. https://doi.org/10.1016/j.earscirev.2010.02.005

Latrubesse E M, Silva SAF, Cozzuol M, Absy ML (2007) Late Miocene continental sedimentation in southwestern Amazonia and its regional significance: biotic and geological evidence. J South Am Earth Sci 23:61–80. https://doi.org/10.1016/j.jsames.2006.09.021

Maynard Smith JM, Savage RJG (1956) Some locomotory adaptations in mammals. Zool J Linn Soc 42:603–622. https://doi.org/10.1111/j.1096-3642.1956.tb02220.x

McEvoy JS (1982) Comparative myology of the pectoral and pelvic appendages of the North American porcupine (*Erethizon dorsatum*) and the prehensile-tailed porcupine (*Coendou prehensilis*). Bull Am Mus Nat Hist 173:337–421.

Millien V (2008) The largest among the smallest: the body mass of the giant rodent *Josephoartigasia monesi*. Proc R Soc B 275(1646) 1953-1955 https://doi.org/10.1098/rspb.2008.0087

Millien V, Bovy H (2010) When teeth and bones disagree: body mass estimation of a giant extinct rodent. J Mammal, 91(1):11–18. https://doi.org/10.1644/08-MAMM-A-347R1.1

Mones A (1980) Un neoepiblemidae del Plioceno medio (Formación Urumaco) de Venezuela (Mammalia: Rodentia: Caviomorpha). Ameghiniana 17:277–279

Mones A (1997) Estudios sobre la familia Dinomyidae. II. Aportes para una osteología comparada de *Dinomys branickii* Peters, 1873 (Mammalia, Rodentia). Comunicaciones Paleontológicas del Museo de Historia Natural de Montevideo 29:1–39.

Mones A, Ojasti J (1986) *Hydrochoerus hydrochaeris*. Mamm Species 246:1–7.

Montalvo CI, Bisceglia S, Kin MS, Sosa RA (2012) Taphonomic analysis of rodent bone accumulations produced by Geoffroy's cat (*Leopardus geoffroyi*, Carnivora, Felidae) in Central Argentina. J Archaeol Sci 39(7):1933–1941 https://doi.org/10.1016/j.jas.2012.02.024.

Montalvo CI, Tallade P (2009) Taphonomy of the accumulations produced by *Caracara plancus* (Falconidae). Analysis of prey remains and pellets. Journal of Taphonomy 7:235–248.

Morgan CC (2009) Geometric morphometrics of the scapula of South American caviomorph rodents (Rodentia: Hystricognathi): form, function and phylogeny. Mammal Biol 74: 497–506. https://doi.org/10.1016/j.mambio.2008.09.006

Morgan CC, Verzi DH (2006) Morphological diversity of the humerus of the South American subterranean rodent *Ctenomys* (Rodentia, Ctenomyidae). J Mammal 87: 1252–1260. https://doi.org/10.1644/06-MAMM-A-033R1.1

Müller RT, Ferreira JD, Pretto FA, Bronzati M, Kerber L (2020) The endocranial anatomy of *Buriolestes schultzi* (Dinosauria: Saurischia) and the early evolution of brain tissues in sauropodomorph dinosaurs. J Anat online first. https://doi.org/10.1111/joa.13350

Muñoz N.A. (2021) Locomotion in rodents and small carnivorans: Are they so different? J Mamm Evol 28: 87–98. https://doi.org/10.1007/s10914-020-09515-8

Muñoz NA., Toledo N, Candela AM, Vizcaíno, S.F (2019) Functional morphology of the forelimb of Early Miocene caviomorph rodents from Patagonia. Lethaia 52 91–106. https://doi.org/10.1111/let.12292

Nasif N, Candela AM, Rasia L, Jaén MCM, Bonini R (2013) Actualización del conocimiento de los roedores de la Mesopotamia Argentina: aspectos sistemáticos, evolutivos y paleobiogeográficos. Asociación Paleontológica Argentina - Publicación Especial 14:153–169.

Negri FR, Bocquentin-Villanueva J, Ferigolo J, Antoine P-O (2010) A review of Tertiary mammal faunas and birds from western Amazonia. In: Hoorn C, Wesselingh FP (eds) Amazonia: Landscapes and Species Evolution: A Look into the Past. Wiley- Blackwell, Oxford, pp 245–258.

Negri FR, Ferigolo J (1999) Anatomia craniana de *Neoepiblema ambrosettianus* (Ameghino, 1889) (Rodentia, Caviomorpha, Neoepiblemidae) do Mioceno superior-Plioceno, Estado do Acre, Brasil, e revisão das espécies do gênero. Bol Mus Para Emílio Goeldi Ciênc 10:1–80.

Paula Couto C (1978) Fossil mammals from the Cenozoic of Acre, Brazil. 2. Rodentia Caviomorpha Dinomyidae. Iheringia – Ser Geol 5:3–17.

Rasia LL, Candela AM (2018) Reappraisal of the giant caviomorph rodent *Phoberomys burmeisteri* (Ameghino, 1886. from the late Miocene of northeastern Argentina, and the phylogeny and diversity of Neoepiblemidae. Hist Biol 30(4):486–495. https://doi.org/10.1080/08912963.2017.1294168

Rasia LL Candela AM (2019) Upper molar morphology, homologies and evolutionary patterns of chinchilloid rodents (Mammalia, Caviomorpha). J Anat 234, 50–65. https://doi.org/10.1111/joa.12895

Rasia LL Candela AM Cañon C (2021) Comprehensive total evidence phylogeny of chinchillids (Rodentia, Caviomorpha): Cheek teeth anatomy and evolution. J Anat. https://doi.org/10.1111/joa.13430

Ribeiro AM, Madden RH, Negri FR, Kerber L, Hsiou AS, Rodrigues KA (2013) Mamíferos fósiles y biocronología en el suroeste de la Amazonia, Brasil. Asociación Paleontológica Argentina – Publicación Especial 14:207–221.

Roach N (2017) *Dinomys branickii*. The IUCN Red List of Threatened Species 2017: e.T6608A22199194. https://dx.doi.org/https://doi.org/10.2305/IUCN.UK.2017-2.RLTS.T6608A22199194.en.

Roach N, Kennerley R (2016a) *Chinchilla lanigera* (errata version published in 2017). The IUCN Red List of Threatened Species 2016: e.T4652A117975205. https://doi.org/10.2305/IUCN.UK.2016-2.RLTS.T4652A22190974.en.

Roach N, Kennerley R (2016b) *Chinchilla chinchilla*. The IUCN Red List of Threatened Species 2016: e.T4651A22191157. https://doi.org/10.2305/IUCN.UK.2016-2.RLTS.T4651A22191157.en.

Rocha-Barbosa O, Loguercio MFC, Renous S, Gasc J-P (2007) Comparative study on the forefoot and hindfoot intrinsic muscles of some cavioidea rodents (Mammalia, Rodentia). Zoology 110:58–65. https://doi.org/10.1016/j.zool.2006.05.002.

Rose KD, Chinnery BJ (2004) The postcranial skeleton of early Eocene rodents. Bull Carnegie Museum Natural Hist 36:211–244.

Samuels JX, Van Valkenburgh B (2008) Skeletal indicators of locomotor adaptations in living and extinct rodents. J Morphol 269:1387–1411. https://doi.org/10.1002/jmor.10662

Sánchez-Villagra MR, Aguilera O, Horovitz I (2003) The anatomy of the world's largest extinct rodent. Science, 301(5640):708–1710. https://doi.org/10.2992/0145-9058(2004)36/211:TPSOEE/2.0.CO;2

Sargis EJ. 2002a. Functional morphology of the forelimb of tupaiids (Mammalia. Scandentia) and its phylogenetic implications. J Morphol 253:10–42. https://doi.org/10.1002/jmor.1110

Sargis EJ. 2002b. Functional morphology of the hindlimb of tupaiids (Mammalia. Scandentia) and its phylogenetic implications. J Morphol 254:149–185. https://doi.org/10.1002/jmor.10025

Stein B (1988) Morphology and allometry in several genera of semiaquatic rodents (*Ondatra*, *Nectomys*, and *Oryzomys*). J Mammal 69:500–511. https://doi.org/10.2307/1381341

Taylor ME. 1974. The functional anatomy of the hindlimb of some African Viverridae (Carnivora). J Morphol 143:307–336. https://doi.org/10.1002/jmor.1051480208

Tejada-Lara JV, Salas-Gismondi R, Pujos F, Baby P, Benammi M, Brusset S, De Franceschi D, Espurt N, Urbina M, Antoine P-O (2015) Life in proto-Amazonia Middle Miocene mammals from the Fitzcarrald Arch (Peruvian Amazonia). Palaeontology 58:341–378. https://doi.org/10.1111/pala.12147

Van Valkenburgh B (1987) Skeletal indicators of locomotor behavior in living and extinct carnivores. J Vert Pal 7:162–182. https://doi.org/10.1080/02724634.1987.10011651

Venables WN, Ripley BD (2002) Modern Applied Statistics with S. New York, Springer.

Vizcaíno SF, Farina RA, Mazzetta GV (1999) Ulnar dimensions and fossoriality in armadillos. Acta Theriol 44:309–320.

Vizcaíno SF, Bargo MS, Cassini GH, Toledo N (2016) Forma y función en paleobiología de vertebrados. La Plata, Editorial de la Universidad Nacional de La Plata (EDULP).

Vucetich MG, Carlini AA, Aguilera O, Sánchez-Villagra MR (2010) The tropics as reservoir of otherwise extinct mammals: the case of rodents from a new Pliocene faunal assemblage from northern Venezuela. J Mamm Evol Paleontol 17:265–273. https://doi.org/10.1007/s10914-010-9142-x

Vucetich MG, Arnal M, Deschamps CM, Perez ME (2015) A brief history of caviomorph rodents as told by the fossil record. In: Vassallo A, Antonucci D (eds) Biology of Caviomorph Rodents; Diversity and Evolution. Sociedad Argentina para el estudio de los Mamíferos, Buenos Aires, pp 11–62

Weisbecker V, Schimid S (2006) Autopodial skeletal diversity in hystricognath rodents: Functional and phylogenetic aspects. Mammal Biol 71(1):27–44. https://doi.org/10.1016/j.mambio.2006.03.005

Wilson LAB, Geiger M (2015) Diversity and evolution of femoral variation in Ctenohystrica. In: Cox, PG, Hautier L (eds) Evolution of the Rodents. Cambridge University Press, Cambridge, pp 510–538.

Woods CA (1972) Comparative myology of jaw, hyoid, and pectoral appendicular regions of New and Old World hystricomorph rodents. Bull Am Mus Nat 147:115–198.